Semisynthetic glycopeptide antibiotics

Groesen, E. van

Chapter 2 |

The guanidino lipoglycopeptides – the development and potent *in vitro* antibacterial activity

Parts of this chapter are under revision as manuscript at *Science Translation Medicine* as:

van Groesen, E., Kotsogianni, I., Arts, M., Tehrani, K.M.H.E., Wade, N., Zwerus, J.T., De Benedetti, S., Bakker, A., Chakraborty, P., van der Stelt, M., Scheffers, D-J., Holden, K., Schneider, T., Martin, N.I. The guanidino lipoglycopeptides: Novel semisynthetic glycopeptides with potent *in vitro* and *in vivo* antibacterial activity. (2022)

Part of the data in this chapter are part of a Dutch Patent:

"Antibacterial Compounds"; Martin, N.I.; van Groesen, E.; Tehrani, K.H.M.E.; Wade, N.; Priority date 24 September 2019; granted 2021; N2023883

2.1 Introduction

Antimicrobial resistance (AMR) poses a major threat to human health and is driven by the rise in multidrug-resistant (MDR) bacteria coupled with the steep decrease in antibiotic drug discovery.[1,2] Infections with Gram-positive pathogens such as methicillin-resistant *Staphylococcus aureus* (MRSA) are increasingly responsible for both community and hospital-acquired infections that result in significant morbidity and mortality.[1–4] For many years the glycopeptide antibiotic vancomycin (**1**) (**Fig. 1**) has been used to effectively treat infections due to MRSA and other Gram-positive pathogens. Today, however, vancomycin-resistant clinical isolates are progressively becoming more common. These strains include vancomycin-intermediate *S. aureus* (VISA) with a minimum inhibitory concentration (MIC) of 4-8 μg/mL, heteroresistant VISA which is largely susceptible with a subpopulation of resistant species, and still relatively rare vancomycin-resistant *S. aureus* (VRSA) with a MIC of ≥16 μg/mL.[3,4] In addition to the increasing difficulties faced in treating *S. aureus* infections, vancomycin-resistant enterococci (VRE) have emerged as a serious clinical challenge against which vancomycin is of no use. It is currently estimated that 30% of all healthcare-associated enterococcal infections are resistant to vancomycin.[2] As noted in the 2019 CDC report on AMR, infections due to MRSA and VRE total nearly 400,000 per year and account for half of all AMR-associated deaths in the United States.[2] In Europe, MRSA and VRE cause approximately 170,000 infections annually and are implicated in 25% of the total AMR-related deaths.[5] In more recent studies, AMR accounted for 1.27 million deaths worldwide in 2019, with drug-resistant Gram-positive species *S. aureus* and *S. pneumoniae* alone being responsible for a combined 0.5 million annual deaths.[6]

In susceptible strains, vancomycin targets the cell wall precursor lipid II by binding to the D-Ala-D-Ala terminus of the pentapeptide via a defined network of five hydrogen bonds. This interaction effectively sequesters lipid II and prevents it from being further incorporated into the growing peptidoglycan by bacterial transpeptidases and transglycosylases, which in turn leads to inhibition of cell wall biosynthesis. This interference with peptidoglycan polymerization results in compromised bacterial cell wall integrity and subsequent cell lysis.[7–10] High levels of resistance to vancomycin is achieved via target modification, wherein the D-Ala-D-Ala termini of peptidoglycan intermediates are mutated to D-Ala-D-Lac/Ser. The introduction of the corresponding depsipeptide motif results in loss of one hydrogen bond and repulsive electrostatic interactions, which are associated with a >1,000-fold reduction in binding affinity rendering vancomycin ineffective.[11,12] Resistance to vancomycin is predominantly due to acquisition of the *vanA* and *vanB* gene clusters leading to D-Ala-D-Lac incorporation.[13,14] However, reduced vancomycin susceptibility can also occur in the absence of a dedicated gene cluster. Such vancomycin-intermediate and -resistant strains are instead characterized by a thickened

cell wall and decreased autolytic activity leading to an increased abundance of D-Ala-D-Ala motifs that effectively trap vancomycin and in doing so allow for the continued growth of the peptidoglycan layer.[3,7,15,16]

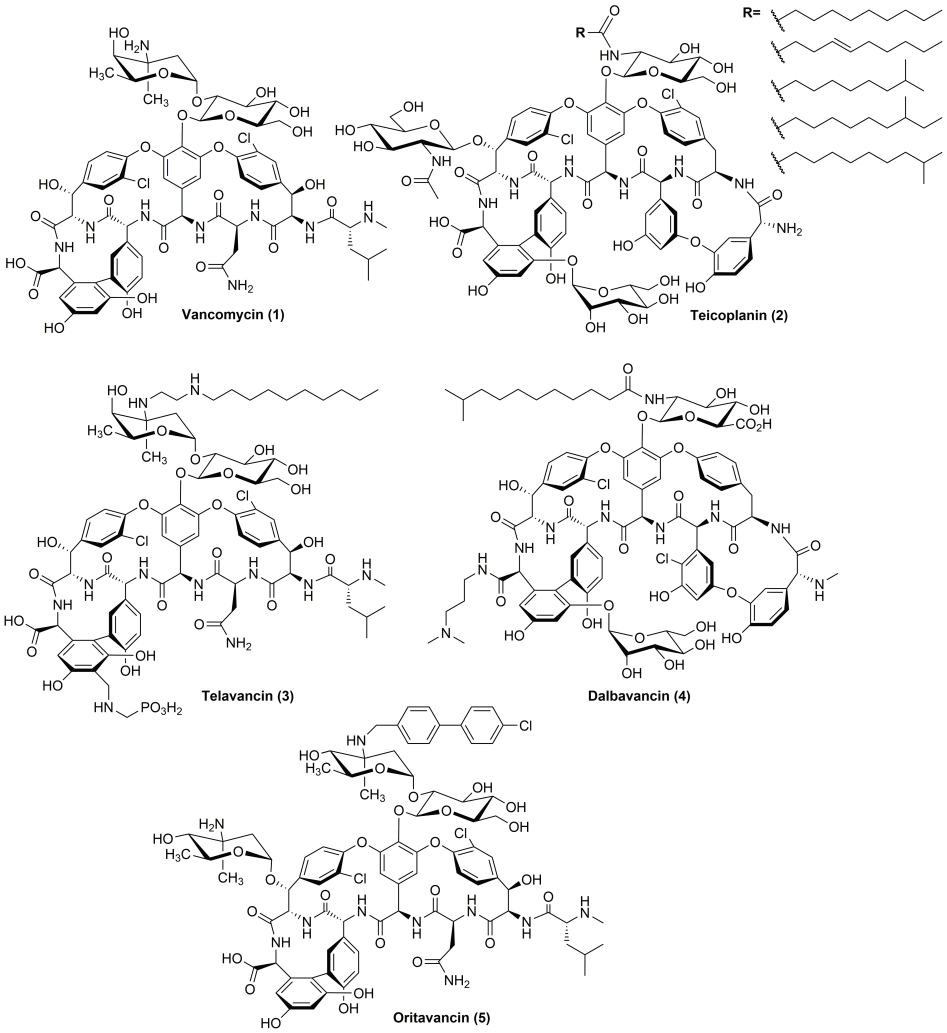

Fig. 1. Structure of clinically used glycopeptide antibiotics

In response to the rapid rise of vancomycin resistance, the lipopeptide daptomycin and the oxazolidinone linezolid were both introduced to the clinic in the early 2000s. However, strains of MRSA and VRE resistant to both antibiotics arose shortly thereafter.[17–20] In parallel, next generation glycopeptide antibiotics were also actively pursued starting with the natural product teicoplanin (**2**) (**Fig. 1**), a mixture of five

chemical species (A_2-1 through A_2-5), which was approved for use in Europe in 1998 but is not used in the North American market.[9] The structure of teicoplanin differs from that of vancomycin, most notably due to the presence of a hydrophobic acyl tail that is associated with its enhanced antibacterial activity. This in turn spawned interest in semisynthetic lipoglycopeptides including telavancin (**3**), dalbavancin (**4**), and oritavancin (**5**) (**Fig. 1**), which were all subsequently developed and approved for clinical use between 2009 and 2014.[9] While these semisynthetic glycopeptides exhibit more potent antibiotic activity than vancomycin, telavancin was recently issued a black-box warning from the FDA due to its associated toxicity concerns.[21] In addition, dalbavancin and oritavancin display unusual pharmacokinetic (PK) properties with half-lives in the order of multiple days. Although this allows for advantageous single or weekly dosing, adverse reactions to the lipoglycopeptides may also persist for weeks before the drug is fully eliminated from the body [22–24] Furthermore, these semisynthetic lipoglycopeptides are known to have poor aqueous solubility,[25,26] a practical yet important characteristic for clinically used agents. Therefore, the development of new glycopeptide antibiotics with enhanced antibacterial activity along with improved PK and safety profiles continues to be of great importance.

A number of strategies have been described in recent years for pursuing glycopeptide antibiotics with enhanced properties.[9,27–45] These strategies range from total synthesis approaches aimed at backbone modification of vancomycin to overcome resistance,[28–32,42,45] to semisynthetic strategies typically involving the introduction of positively charged motifs and/or hydrophobic moieties[27,33–35,37–42] as well as antibiotic-hybrids.[35,43,44] In considering these various approaches, we were particularly intrigued by reports describing the introduction of positively charged functional groups at the vancosamine moiety in vancomycin as a means of improving antibacterial activity.[38,39] Given our group's expertise in the synthesis of biologically active compounds containing substituted guanidine groups,[46–49] we hypothesized that the introduction of an appropriately substituted guanidinium motif at the vancosamine site in vancomycin might provide access to novel semisynthetic glycopeptides with enhanced properties.

In the present study, we report the development of a panel of novel semisynthetic vancomycin derivatives containing lipidated guanidine moieties. These guanidino lipoglycopeptides are readily synthesized from vancomycin in a two-step process and possess unique properties owing to the presence of both a hydrophobic lipid tail and a polar guanidine group. At physiological pH, the guanidine moiety is fully protonated, providing a highly delocalized positive charge that also promotes increased aqueous solubility. To date, no such guanidino lipoglycopeptides have been reported. The guanidino lipoglycopeptides display potent activity *in vitro* against a variety of Gram-positive bacteria, including vancomycin-resistant strains.

2.2 Results and Discussion

2.2.1 Design and synthesis of the guanidino lipoglycopeptides

The synthetic route devised for the preparation of the guanidino lipoglycopeptides relies upon selective modification of the vancosamine nitrogen in vancomycin by means of reductive amination (see **Scheme S1** for the synthetic route), a known and reliable method for accessing vancomycin analogues.[9,38] The aldehyde building blocks required to introduce the lipidated guanidine moiety were prepared using a robust and modular building block approach. Specifically, the lipophilic substituted guanidino group was first prepared as the corresponding allyl carbamate protected species and linked to an aromatic aldehyde providing the reactive handle for the key reductive amination step. Following the reductive amination and subsequent alloc-group removal, the guanidino lipoglycopeptides were purified by high performance liquid chromatography (HPLC). Via this route, guanidino lipoglycopeptides **6-20** were prepared incorporating a diverse panel of lipophilic fragments: e.g. linear, branched, unsaturated, aromatic substituents (**Fig. 2**).

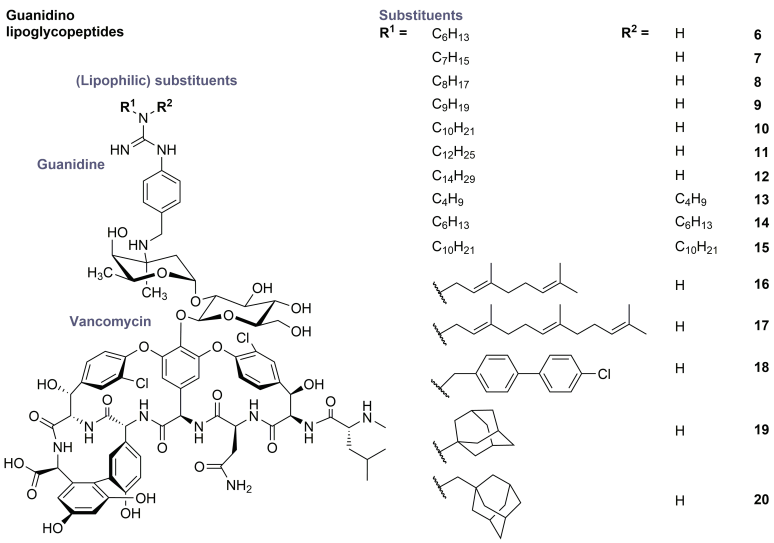

Fig. 2. **Structures of guanidino lipoglycopeptides 6-20 prepared in the present study**

2.2.2 *In vitro* antibacterial activity against Gram-positive strains

The antibacterial activities of guanidino lipoglycopeptides **6-20** were assessed in broth microdilution assays. Most of the compounds are highly effective against an initial panel of Gram-positive pathogens with activities superior to vancomycin and the other clinically used glycopeptide antibiotics (**Table 1**). Notably, the most potent compounds identified are >100-fold more active than vancomycin against methicillin-sensitive *S. aureus* (MSSA) and MRSA and even ≥1,000-fold more active against VISA. Furthermore, the guanidino lipoglycopeptides also outperform clinically used semisynthetic lipoglycopeptides. Specifically, against MRSA and VISA, the most active guanidino lipoglycopeptides exhibit MICs >8-fold and >30-fold lower than those observed for the most potent clinically used glycopeptides (oritavancin and telavancin respectively). In addition, most of the guanidino lipoglycopeptides are ≥100-fold more active than vancomycin against VRSA, with some compounds showing enhancements as high as 2,000-fold. In the case of VRE with the VanA phenotype, the guanidino lipoglycopeptides show increased potencies of up to a 1,000-fold compared to vancomycin while against VanB-type VRE isolates enhancements of as high as 16,000-fold are observed. In addition, the most potent guanidino lipoglycopeptides are >50-fold more active than vancomycin against vancomycin-sensitive enterococci (VSE) and *S. pneumoniae*. The guanidino lipoglycopeptides were further assessed against a broader panel of MRSA, VISA, VRSA, and VRE (*E. faecalis)* strains, which again demonstrated their superior activity relative to vancomycin and equipotent or superior activity to the other clinically relevant glycopeptides (**Table S1**). Six of the most potent guanidino lipoglycopeptides (compounds **7-9**, **14**, **16**, and **18**) were also selected for further assessment against 31 different VRE isolates revealing MIC_{50} and MIC_{90} values ranging from 0.031-1.0 μg/mL and 0.5-8.0 μg/mL respectively (**Table 2**). Additionally, against an expanded panel of VISA and VRSA strains compounds **7**, **14** and **18** are consistently more active than vancomycin, and equipotent or superior to telavancin (**Table 3**).

Table 1. *In vitro* activity of the guanidino lipoglycopeptides against Gram-positives.

		MIC (μg/mL)							
Compound		**Strain**							
Id	**Structure**	**MSSA[a]**	**MRSA[b]**	**VISA[c]**	**VRSA[d]**	**VSE[e]**	**VRE[f] VanA**	**VRE[g] VanB**	**S. P.[h]**
1	Vancomycin	1	1	8	>128	0.5	>128	128	0.5
2	Teicoplanin	0.5	0.5	16	32	0.5	>128	0.25	0.031
3	Telavancin	0.125	0.125	0.25	4	0.016	4	≤0.008	≤0.008
4	Dalbavancin	0.25	0.25	1	16	0.063	128	0.016	≤0.008
5	Oritavancin	0.25	0.063	1	0.25	0.063	0.5	0.125	≤0.008
Guanidino lipoglycopeptides									
6	-C_6H_{13}	0.063	0.063	0.25	4	0.031	8	0.031	0.016
7	-C_7H_{15}	≤0.008	0.016	0.031	1	≤0.008	4	≤0.008	≤0.008
8	-C_8H_{17}	≤0.008	≤0.008	≤0.008	0.5	0.016	1	≤0.008	≤0.008
9	-C_9H_{19}	0.016	≤0.008	≤0.008	0.125	0.031	0.5	≤0.008	≤0.008
10	-$C_{10}H_{21}$	0.016	0.063	0.016	0.063	0.016	0.25	≤0.008	≤0.008
11	-$C_{12}H_{25}$	0.125	0.5	0.5	0.125	0.125	0.125	0.031	≤0.008
12	-$C_{14}H_{29}$	2	4	4	0.5	0.5	0.5	0.5	0.031
13	-$(C_4H_9)_2$	0.125	0.125	0.5	16	0.063	32	0.5	0.063
14	-$(C_6H_{13})_2$	≤0.008	0.063	≤0.008	0.25	≤0.008	1	≤0.008	≤0.008
15	-$(C_{10}H_{21})_2$	16	16	32	8	4	8	4	2
16	-Ger[i]	≤0.008	0.031	≤0.008	0.063	≤0.008	1	≤0.008	≤0.008
17	-Far[j]	0.031	0.063	0.125	0.125	0.031	0.125	0.016	≤0.008
18	-CH_2-CBP[k]	0.016	0.031	0.016	0.063	≤0.008	0.125	≤0.008	≤0.008
19	-TCD[l]	0.016	0.031	0.125	8	≤0.008	8	0.016	0.016
20	-CH_2-TCD[l]	≤0.008	≤0.008	0.016	2	≤0.008	2	≤0.008	≤0.008

MIC values are the median of a minimum of triplicates. MIC = minimum inhibitory concentration. [a]ATCC29213. [b]Methicillin-resistant *S. aureus* USA300. [c]Vancomycin-intermediate *S. aureus* LIM-2, NR-45881. [d]Vancomycin-resistant (VanA) *S. aureus* HIP13419, NR-46413. [e]Vancomycin-sensitive *Enterococcus faecium* E980. [f]Vancomycin-resistant (VanA) *E. faecium* E155. [g]Vancomycin-resistant (VanB) *E. faecium* E7314. [h]*Streptococcus pneumoniae* 153, ATCC6305. [i]Ger = Geranyl. [j]Far = Farnesyl. [k]CBP = 4-chloro-1,1'-biphenyl. [l]TCD = Tricyclo[3.3.1.1^{3,7}]decane or adamantane

Table 2. MIC, MIC_{50}, and MIC_{90} of the guanidino lipoglycopeptides against 31 vancomycin-resistant *E. faecium* strains. The MIC_{50} and MIC_{90} correspond to the concentrations at which growth was visibly inhibited for 50% and 90% of the strains tested respectively.

		MIC (µg/mL)							
Enterococci		**Compounds**							
Strain Id	**Van-type**	Vancomycin **(1)**	Telavancin **(3)**	**7**	**8**	**9**	**14**	**16**	**18**
E155	VanA	>128	4	2	1	0.5	1	1	0.125
E0013	VanA	>128	4	4	1	0.5	2	2	0.25
E0072	VanA	>128	2	0.25	0.5	0.125	0.25	0.5	≤0.008
E0300	VanA	>128	8	4	2	0.5	1	4	0.25
E0321	VanA	>128	16	8	4	1	2	8	0.5
E0333	VanA	>128	8	8	4	1	2	8	0.5
E0338	VanA	>128	8	4	2	0.5	2	4	0.125
E0341	VanA	>128	8	8	4	1	2	4	0.25
E0506	VanA	>128	4	2	2	0.5	1	2	0.125
E0745	VanA	>128	4	1	0.25	0.125	0.25	1	0.031
E1130	VanA	>128	≤0.008	≤0.008	≤0.008	≤0.008	≤0.008	≤0.008	≤0.008
E1441	VanA	>128	8	4	2	1	2	4	0.5
E1679	VanA	>128	16	16	8	4	8	16	1
E1763	VanA	128	1	0.25	0.031	≤0.008	0.031	0.125	≤0.008
E2297	VanA	>128	4	2	1	0.5	1	2	0.125
E2359	VanB	128	≤0.008	≤0.008	≤0.008	≤0.008	≤0.008	≤0.008	≤0.008
E2365	VanB	16	≤0.008	≤0.008	≤0.008	≤0.008	≤0.008	≤0.008	≤0.008
E2373	VanA	>128	8	4	2	0.5	1	4	0.25
E6016	VanA	>128	4	1	0.5	0.25	0.5	2	0.063
E7312	VanA	>128	2	0.25	0.063	0.031	0.125	0.25	0.016
E7314	VanB	128	≤0.008	≤0.008	≤0.008	≤0.008	≤0.008	≤0.008	≤0.008
E7319	VanA	>128	8	0.5	0.125	0.063	0.25	0.5	0.031
E7329	VanA	1	≤0.008	≤0.008	≤0.008	≤0.008	≤0.008	≤0.008	≤0.008
E7401	VanB	16	≤0.008	≤0.008	≤0.008	≤0.008	≤0.008	≤0.008	≤0.008
E7403	VanB	16	≤0.008	≤0.008	≤0.008	≤0.008	≤0.008	≤0.008	≤0.008
E7413	VanA	>128	8	8	4	2	2	8	0.5
E7424	VanB	4	≤0.008	≤0.008	≤0.008	≤0.008	≤0.008	≤0.008	≤0.008
E7464	VanB	16	≤0.008	≤0.008	≤0.008	≤0.008	≤0.008	≤0.008	≤0.008
E8218	VanB	8	≤0.008	≤0.008	≤0.008	≤0.008	≤0.008	≤0.008	≤0.008
E8235	VanB	16	≤0.008	≤0.008	≤0.008	≤0.008	≤0.008	≤0.008	≤0.008
E8237	VanA	>128	16	8	2	1	2	4	0.25
MIC_{50}		128	4	1	0.5	0.125	0.25	1	0.031
MIC_{90}		128	8	8	4	1	2	8	0.5

MIC values are the median of a minimum of triplicates. MIC = minimum inhibitory concentration. In cases were >128 was the MIC, 128 µg/mL was used in the calculation of the MIC_{50} and MIC_{90}. The real value is higher. In cases where ≤0.008 was the MIC, 0.008 µg/mL was used in the calculation of the MIC_{50} and MIC_{90}. The real value could be lower.

Table 3. MIC, MIC_{50}, and MIC_{90} of the guanidino lipoglycopeptides against a panel of vancomycin-resistant and -intermediate *S. aureus* strains. The MIC_{50} and MIC_{90} correspond to the concentrations at which growth was visibly inhibited for 50% and 90% of the strains tested respectively.

		MIC (μg/mL)					
VRSA/VISA		**Compounds**					
Strain Id		Vancomycin **(1)**	Telavancin **(3)**	Oritavancin **(5)**	**7**	**14**	**18**
Vancomycin-resistant *Staphylococcus aureus*							
VRS1		>128	8	1	16	4	0.5
VRS2		32	2	0.25	0.25	≤0.016	≤0.016
VRS3a		64	1	0.5	0.25	≤0.016	≤0.016
VRS3b		>128	4	0.25	1	0.25	0.063
VRS4		>128	4	1	8	2	0.25
VRS5		>128	4	0.5	4	1	0.25
VRS7		>128	4	0.5	4	2	0.25
VRS8		>128	16	1	16	4	1
VRS9		>128	16	2	16	4	1
VRS11a		>128	8	1	16	4	1
VRS11b		>128	8	1	16	4	1
NRS63SH		>128	8	1	8	2	0.5
BR-VRSA		>128	8	0.25	4	1	0.5
Vancomycin-intermediate *Staphylococcus aureus*							
NRS17		8	1	4	0.25	0.5	0.25
NRS18		8	0.25	1	0.125	0.25	0.063
NRS19		4	0.25	1	0.063	0.25	0.063
NRS51		4	0.125	0.5	0.031	0.125	0.016
NRS52		4	0.25	0.5	0.031	0.031	0.016
NRS402		8	0.25	4	0.063	0.063	0.031
LIM-2		8	0.25	1	0.031	≤0.008	0.016
VRSA	MIC_{50}	128	8	1	8	2	0.5
	MIC_{90}	128	16	1	16	4	1
VISA	MIC_{50}	8	0.25	1	0.063	0.125	0.031
	MIC_{90}	8	1	4	0.25	0.5	0.25
Both	MIC_{50}	128	4	1	4	1	0.25
	MIC_{90}	128	16	4	16	4	1

MIC values are the median of a minimum of triplicates. MIC = minimum inhibitory concentration. In cases where the MIC was >128, 128 μg/mL was used in the calculation of the MIC_{50} and MIC_{90}. The real value is higher. In cases where the MIC was ≤0.008 or ≤0.016, 0.008 μg/mL and 0.016 μg/mL were respectively used in the calculation of the MIC_{50} and MIC_{90}. The real value could be lower.

2.2.3 *In vitro* antibacterial activity against anaerobic *Clostridia*

Guanidino lipoglycopeptides **7**, **14**, and **18** were also assessed against anaerobic *Clostridium* species (**Table 4**). Vancomycin is the standard of care for *Clostridium* infections,[50] but resistance to vancomycin has been reported.[51,52] Antibiotic treatment in humans allows for the anaerobic species to colonize the gut, of which *Clostridium difficile* is one of the most important healthcare-associated pathogens causing antibiotic-induced diarrhea (ADD).[51,52] *C. difficile* caused 12,000 deaths in the US alone and is the only Gram-positive pathogen indicated as urgent threat by the CDC.[2] Furthermore, *C. difficile* is also involved in community-associated infections.[2] In addition to *C. difficile,* one of the second largest causes of ADD is caused by *C. perfringens.*[53] Besides healthcare-associated problems, many *Clostridium* species are responsible for food spoilage, such as *C. tyrobutyricum*[54] and *C. botulinum*,[55] of which the latter is responsible for food-born botulism causing severe intoxication by deadly botulinum neurotoxin production and was therefore substituted for the highly resembling *C. sporogenes* in MIC assays.[55,56]

Table 4. *In vitro* activity of the guanidino lipoglycopeptides against *Clostridia*.

		MIC (µg/mL)						
Clostridia		**Compounds**						
Species	**Strain Id**	Vancomycin (**1**)	Telavancin (**3**)	Dalbavancin (**4**)	Oritavancin (**5**)	**7**	**14**	**18**
C. difficile	DSMZ27543	6.25	3.13	1.56	0.78	0.25	0.50	0.50
C. perfringens	SM101	1.56	3.13	3.13	0.78	0.13	0.5	0.25
	VWO031	1.56	1.56	0.78	1.56	0.06	0.5	0.25
	C202	3.13	0.78	0.23	3.13	0.25	0.5	0.5
	C198	6.25	6.25	1.56	1.56	0.06	0.5	0.13
	VWA080	3.13	1.56	0.39	1.56	0.03	0.5	0.25
	VWA009	6.25	6.25	3.13	1.56	0.03	0.5	0.13
C. sporogenes	ADRIAS882	12.5	3.13	1.56	1.56	0.25	1	1
	ATCC25579	6.25	1.56	0.39	1.56	0.03	0.5	0.13
	ATCC3584	12.5	1.56	1.56	3.13	0.13	1	0.5
C. tyrobutyricum	DSM663	3.13	1.56	1.56	1.56	0.25	0.5	0.5
	S46	12.5	0.2	0.2	0.78	0.13	1	0.13
	NIZO570	12.5	0.78	1.56	1.56	0.25	1	1
	NIZO575	12.5	1.56	0.78	1.56	0.5	1	1

MIC values are the median of a minimum of triplicates. MIC = minimum inhibitory concentration. *Experiment performed by Nils Leibrock at NIZO.*

While the MIC of the clinically used glycopeptide antibiotics against *C. difficile* ranged from 6.25 µg/mL (vancomycin) to 0.78 µg/mL (oritavancin), the guanidino lipoglycopeptides had superior activity with MIC values of 0.5 µg/mL for **14** and **18**, and even 0.25 µg/mL for **7**. Furthermore, against a panel of *C. perfringens, C. sporogenes,*

and *C. tyrobutyricum* strains, all three guanidino lipoglycopeptides consistently outperformed the clinically used glycopeptide antibiotics, with compound **7** having the most potent activity with MIC values as low as 0.03 μg/mL against *C. perfringens* and *C. sporogenes* and 0.13 μg/mL against *C. tyrobutyricum*.

2.2.4 *In vitro* antibacterial activity against Gram-negative strains

Previous research has demonstrated the potential for covalently modified semi-synthetic glycopeptide antibiotics, such as vancomycin and teicoplanin, to be repurposed to effectively target Gram-negative species as well.[33–36,43,44,57,58] However, similar to all clinically used glycopeptides, the guanidino lipoglycopeptides exhibit no significant activity against Gram-negative bacteria (**Table 5**).

Table 5. *In vitro* activity of the guanidino lipoglycopeptides against Gram-negatives.

	MIC (μg/mL)							
Gram-negatives	**Compounds**							
Strain Id	Vancomycin (**1**)	Telavancin (**3**)	**7**	**8**	**9**	**14**	**16**	**18**
E. coli								
ATCC 35218	>128	>128	>128	>128	>128	>128	>128	>128
ATCC 25922	>128	>128	>128	>128	>128	>128	>128	>128
W3110	>128	>128	>128	>128	>128	>128	>128	>128
K. pneumoniae								
ATCC 13883	>128	>128	>128	>128	>128	>128	>128	>128
ATCC 27736	>128	>128	>128	>128	>128	>128	>128	>128
JS265	>128	>128	>128	>128	>128	>128	>128	>128

MIC values are the median of a minimum of triplicates. MIC = minimum inhibitory concentration.

2.2.5 Structure-activity relationship

The results of the MIC assays indicate that the guanidino lipoglycopeptides are very active with significant enhancements in activity relative to vancomycin. Notably, analogues containing straight-chain aliphatic lipophilic tails comprising of seven to nine carbon atoms, as in compounds **7**-**9** (heptyl-nonyl), are more potent against MRSA, VISA, and VanB-type VRE strains, whereas the introduction of longer lipid tails, such as for **10** and **11** (decyl, dodecyl), perform better against VanA-type VRSA and VRE. However, when the lipids become longer, such as for **12** (tetradecyl), activity is compromised, as reflected by the reduced potency against MSSA and MRSA where the MIC values measured for **12** are higher than those achieved with vancomycin. On the other hand, the inclusion of shorter lipophilic substituents, as in analogue **6** (hexyl), results in a reduction in activity against vancomycin-resistant strains. Thus, among the aliphatic mono-substituted guanidino lipoglycopeptides, optimal potency appears to be achieved by incorporating a linear lipophilic moiety of seven to twelve carbon atoms. We

also examined the effect of including two substituents on the guanidino moiety, as in compounds **13**-**15**. In this case, a slightly different trend was observed compared with the mono-substituted guanidino lipoglycopeptides: while the C_{10} mono-substituted **10** is clearly more active than the C_6 mono-substituted **6**, for the di-substituted analogues the trend is reversed. Specifically, the C_6 di-substituted system (**14**) is much more potent than the C_{10} di-substituted analogue (**15**), with the latter also having reduced activity compared to vancomycin. In addition to mono- and di-substitution with linear aliphatic moieties, we also explored the introduction of more exotic lipophilic moieties including branched, unsaturated, aromatic, and adamantyl-based substituents (compound **16**-**20**). In general, these analogues are also highly active with **16**-**18** performing particularly well against vancomycin-resistant strains.

2.3 Conclusions

While the need for new therapies to treat Gram-negative infections is of growing concern, the AMR-related morbidity and mortality related to infections caused by Gram-positive pathogens still far exceeds that associated with Gram-negative organisms.[1,2] From the time of their clinical introduction, the glycopeptides have been a cornerstone in the treatment of serious Gram-positive infections. In recent years, semisynthetic lipoglycopeptides such as the clinically approved telavancin, dalbavancin, and oritavancin have proven to be important additions to this arsenal, particularly in light of growing rates of resistance to vancomycin.[9,59] While these next-generation lipoglycopeptides show enhanced antibacterial activity relative to vancomycin, they also possess limitations related to their toxicity as well as their physicochemical and pharmacokinetic properties.[21,22,25,26]

We here report a new class of highly active semisynthetic lipoglycopeptides containing a basic guanidino group bearing a lipophilic substituent. The route developed for the synthesis of the guanidino lipoglycopeptides is flexible and allows for the inclusion of a range of different substituents (**Scheme S1**, **Fig. 2**). A number of compounds prepared following this route were found to exhibit extremely potent *in vitro* antibacterial activity against a panel of aerobic and anaerobic Gram-positive strains (**Table 1**, **Table 4**). In most cases, the MIC values measured for the guanidino lipoglycopeptides are much lower than those measured for vancomycin, typically translating into 100- or 1,000-fold increases in activity and enhancements of >16,000-fold for some vancomycin-resistant strains. In addition, the guanidino lipoglycopeptides were consistently found to exhibit superior or equipotent *in vitro* antibacterial activity relative to the clinically used semisynthetic lipoglycopeptide telavancin.

In summary, we here report the development of the guanidino lipoglycopeptides, a promising new class of semisynthetic glycopeptide antibiotics. The *in vitro* activity studies performed with the guanidino lipoglycopeptides demonstrate the potential of this new class of semisynthetic glycopeptide antibiotics. Further assessment of the guanidino lipoglycopeptides in *in vitro* cell-based studies (such as toxicity, resistance induction, and anti-biofilm activity), mechanistic studies (such as target binding and membrane depolarization studies), and *in vivo* studies (tolerability, PK, and efficacy) is described in **Chapter 3**.

2.4 Experimental Methods

2.4.1 Chemical synthesis

General. Compounds were obtained commercially unless specified otherwise. In cases where the product from a previous reactions was used directly, the equivalents of the other components indicated in the reaction were based on the equivalents used in the previous reaction, assuming quantitative conversion. Thin layer chromatography (TLC) was performed on SiliaPlate TLC plates (SiliCycle, glass-backed, silica, 250 μm). Visualization was done using UV light, ninhydrin stain, permanganate stain or cerium ammonium molybdate stain. Silica gel column chromatography was performed using SiliaFlash® P60 silica gel (SiliCycle). The final compounds were purified by preparative reverse phase high performance liquid chromatography (RP-HPLC) using a Reprosil Gold 120 C18 10 μm column (length: 250 mm, ID: 25 mm. Lot No: 8768. part No: r10.9g.s2525. Serial No: 18020211570. Dr Maisch GmbH) on a BESTA-Technik system equipped with an ECOM Flash UV detector monitoring at 214 nm and SCPA PrepCon 5 software, using a 12 mL/min flow rate. Analytical HPLC to assess compound purity was performed using a Dr. Maisch ReproSil Gold 120 C_{18} column (4.6 × 250 mm, 5 μm) on a Shimadzu Prominence-i LC-2030 system, using a 1 mL/min flow rate at 30 °C. All spectra displayed to show purity were recorded at 214 nm. Buffers used for preparative and analytical HPLC were 50 mM ammonium acetate as buffer A and 95% CH_3CN + 5% H_2O as buffer B unless stated otherwise. Nuclear magnetic resonance (NMR) spectra were obtained from a Bruker DPX-300, super conducting magnet with a field strength of 7.0 Tesla, equipped with 5 mm BBO, Broadband Observe probe head, high resolution with Z- Gradient, and a 5 mm 19F / 1H dual high resolution probe. High resolution mass spectroscopy (HR-MS) analyses were performed on one of two systems: 1) Thermo Scientific Dionex UltiMate 3000 HPLC system with a Phenomenex Kinetex C18 column (2.1 x 150 mm, 2.6 μm) at 35 °C and equipped with a diode array detector. The following solvent system, at a flow rate of 0.3 mL/min, was used: solvent A, 0.1% formic acid in H_2O; solvent B, 0.1% formic acid in CH_3CN. Gradient elution was as follows: 95:5 (A/B) for 1 min, 95:5 to 5:95 (A/B) over 9 min, 5:95 to 2:98 (A/B) over 1 min, 2:98 (A/B) for

1 min, then reversion back to 95:5 (A/B) over 2 min, 95:5 (A/B) for 1 min. This system was connected to a Bruker micrOTOF-Q II mass spectrometer (electrospray ionization) calibrated internally with sodium formate; 2) Shimadzu Nexera X2 UHPLC system with a Waters Acquity HSS C18 column (2.1 × 100 mm, 1.8 μm) at 30 °C and equipped with a diode array detector. The following solvent system, at a flow rate of 0.5 mL/min, was used: solvent A, 0.1% formic acid in H_2O; solvent B, 0.1% formic acid in CH_3CN. Gradient elution was as follows: 95:5 (A/B) for 1 min, 95:5 to 15:85 (A/B) over 6 min, 15:85 to 0:100 (A/B) over 1 min, 0:100 (A/B) for 3 min, then reversion back to 95:5 (A/B) for 3 min. This system was connected to a Shimadzu 9030 QTOF mass spectrometer (ESI ionisation) calibrated internally with Agilent's API-TOF reference mass solution kit (5.0 mM purine, 100.0 mM ammonium trifluoroacetate and 2.5 mM hexakis(1H,1H,3H-tetrafluoropropoxy)phosphazine) diluted to achieve a mass count of 10000.

Synthesis of previously published compounds. **Alloc-NCS** was synthesized according to a previously published synthesis.[60] Synthesis of **4-(1,3-dioxolan-2-yl)aniline** was performed according to a previously described procedure.[61] **(2*E*,6*E*)-3,7,11-trimethyldodeca-2,6,10-trien-1-amine** was synthesized by making the bromide (**(*E*)-1-bromo-3,7-dimethylocta-2,6-diene**) from *trans,trans*-farnesol ((*E*,*E*)-3,7,11-trimethyl-2,6,10-dodecatrien-1-ol) as previously described,[62,63] followed by conversion to the amine according to a published method.[64,65] The synthesis of **(*E*)-3,7-dimethylocta-2,6-dien-1-amine** followed the same literature procedures[64,65] using the commercially available bromide. **4'-Chloro-([1,1'-biphenyl]-4-yl)methanamine** was made according to a published literature procedure.[65]

The synthesis of N-(allyloxycarbonyl)-N'-(4-(1,3-dioxolan-2-yl)phenyl)thiourea. To a crude solution of 4-(1,3-dioxolan-2-yl)aniline (50 mmol, 1 eq) and DIPEA (50 mmol, 1 eq) in DCM, crude Alloc-NCS was added at RT until TLC (in DCM with 5% EtOAc) confirmed complete conversion of 4-(1,3-dioxolan-2-yl)aniline to *N*-(allyloxycarbonyl)-*N'*-(4-(1,3-dioxolan-2-yl)phenyl)thiourea. Crude product was concentrated under reduced pressure and purified by silica gel column chromatography (DCM with increasing gradient up to 5% EtOAc). Yield over 2 steps: 77%. 1H NMR (300 MHz, CDCl3) δ/ppm: 11.47 (s, 1H), 8.42 (s, 1H), 7.67 (d, *J* = 8.5 Hz, 2H), 7.51 (d, *J* = 8.5, 2H), 6.00 – 5.85 (m, 1H), 5.83 (s, 1H), 5.39 (dd, *J* = 17.2, 1.4 Hz, 1H), 5.33 (dd, *J* = 10.4, 1.2 Hz, 1H), 4.70 (dt, *J* = 5.8, 1.3 Hz, 2H), 4.18 – 3.98 (m, 4H). 13C NMR (75 MHz, CDCl3) δ/ppm: 177.75, 152.65, 138.30, 136.59, 130.84, 127.15, 124.10, 119.86, 103.25, 67.37, 65.40. HR-MS: m/z 309.0913 (observed), 309.0909 (calculated for $[M+H]^+$).

*General procedure for the synthesis of **6a-20a**.* To a solution of *N*-(allyloxycarbonyl)-*N'*-(4-(1,3-dioxolan-2-yl)phenyl)thiourea (5.8 mmol, 1 eq) in DCM, the desired amine substituent (11.7 mmol, 2 eq) and NEt_3 (11.7 mmol, 2 eq) were added. Subsequently EDC

HCl (11.7 mmol, 2 eq) was added and the reaction mixture was stirred at RT. After 2 h, the reaction was complete and the solution was concentrated under reduced pressure. The products were purified by silica gel column chromatography (DCM + 5% EtOAc).

*Characterization of **6a***. Yield: Quantitative. ^{1}H NMR (300 MHz, $CDCl_3$) δ/ppm: 10.70 (s, 1H), 7.53 (d, *J* = 8.0 Hz, 2H), 7.22 (d, *J* = 6.8 Hz, 2H), 6.13 – 5.91 (m, 1H), 5.78 (s, 1H), 5.34 (d, *J* = 17.3 Hz, 1H), 5.21 (d, *J* = 10.4 Hz, 1H), 4.62 (d, *J* = 5.6 Hz, 2H), 4.21 – 3.99 (m, 4H), 3.43 – 3.29 (m, 2H), 1.57-1.38 (m, 2H), 1.36-1.16 (m, 6H), 0.94 – 0.78 (m, 3H). ^{13}C NMR (75 MHz, $CDCl_3$) δ/ppm: 164.21, 158.64, 137.02, 136.61, 133.67, 128.33, 117.42, 103.14, 66.02, 65.48, 41.37, 31.45, 29.40, 26.51, 22.54, 14.02. HR-MS: *m/z* 376.2242 (observed), 376.2236 (calculated for $[M+H]^+$)

*Characterization of **7a***. Yield: Quantitative. ^{1}H NMR (300 MHz, $CDCl_3$) δ/ppm: 10.70 (s, 1H), 7.53 (d, *J* = 8.0 Hz, 2H), 7.23 (d, *J* = 7.7 Hz, 2H), 6.14 – 5.93 (m, 1H), 5.79 (s, 1H), 5.34 (dd, *J* = 17.2, 1.3 Hz, 1H), 5.21 (dd, *J* = 10.4, 1.2 Hz, 1H), 4.62 (d, *J* = 5.7 Hz, 2H), 4.22 – 4.00 (m, 4H), 3.42 – 3.29 (m, 2H), 1.57 1.38 (m, 2H), 1.34 – 1.18 (m, 8H), 0.92 – 0.80 (m, 3H).^{13}C NMR (75 MHz, $CDCl_3$) δ/ppm: 164.27, 158.69, 137.10, 136.57, 133.77, 128.40, 117.45, 103.18, 66.06, 65.54, 41.43, 31.77, 29.50, 29.00, 26.85, 22.65, 14.15. HR-MS: *m/z* 390.2402 (observed), 390.2393 (calculated for $[M+H]^+$)

*Characterization of **8a***. Yield: Quantitative. ^{1}H NMR (300 MHz, $CDCl_3$) δ/ppm: 10.70 (s, 1H), 7.53 (d, *J* = 8.0 Hz, 2H), 7.22 (d, *J* = 7.4 Hz, 2H), 6.12 – 5.93 (m, 1H), 5.79 (s, 1H), 5.34 (dd, *J* = 17.2, 1.5 Hz, 1H), 5.21 (dd, *J* = 10.4, 1.4 Hz, 1H), 4.62 (d, *J* = 5.7 Hz, 2H), 4.22 – 3.99 (m, 4H), 3.43 – 3.28 (m, 2H), 1.59 – 1.37 (m, 2H), 1.34 – 1.15 (m, 10H), 0.93 – 0.81 (m, 3H).^{13}C NMR (75 MHz, $CDCl_3$) δ/ppm: 164.23, 158.67, 137.09, 136.55, 133.74, 128.37, 125.51, 117.43, 103.15, 66.04, 65.51, 41.41, 31.82, 29.47, 29.27, 29.21, 26.87, 22.69, 14.16. HR-MS: *m/z* 404.2547 (observed), 404.2549 (calculated for $[M+H]^+$)

*Characterization of **9a***. Yield: Quantitative. ^{1}H NMR (300 MHz, $CDCl_3$) δ/ppm: 10.71 (s, 1H), 7.53 (d, *J* = 7.8 Hz, 2H), 7.22 (d, *J* = 7.2 Hz, 2H), 6.15 – 5.93 (m, 1H), 5.78 (s, 1H), 5.34 (d, *J* = 17.2 Hz, 1H), 5.21 (d, *J* = 10.4 Hz, 1H), 4.61 (d, *J* = 5.5 Hz, 2H), 4.22 – 3.97 (m, 4H), 3.44 – 3.26 (m, 2H), 1.57 – 1.38 (m, 2H), 1.38 – 1.13 (m, 12H), 0.96 – 0.79 (m, 3H). ^{13}C NMR (75 MHz, $CDCl_3$) δ/ppm: 164.14, 158.58, 137.01, 136.45, 133.67, 128.26, 125.38, 117.32, 103.06, 65.93, 65.41, 41.31, 31.81, 29.41, 29.38, 29.23, 29.18, 26.78, 22.63, 14.10. HR-MS: *m/z* 418.2716 (observed), 418.2706 (calculated for $[M+H]^+$)

*Characterization of **10a***. Yield: Quantitative. ^{1}H NMR (300 MHz, $CDCl_3$) δ/ppm: 10.70 (s, 1H), 7.53 (d, *J* = 7.6 Hz, 2H), 7.22 (d, *J* = 7.1 Hz, 2H), 6.11 – 5.92 (m, 1H), 5.79 (s, 1H), 5.34 (d, *J* = 17.2 Hz, 1H), 5.21 (d, *J* = 10.4 Hz, 1H), 4.62 (d, *J* = 5.3 Hz, 2H), 4.22 – 3.99 (m, 4H), 3.43 – 3.28 (m, 2H), 1.56 – 1.38 (m, 2H), 1.36 – 1.14 (m, 14H), 0.92 –

0.82 (m, 3H). ^{13}C NMR (75 MHz, $CDCl_3$) δ/ppm: 164.23, 158.66, 137.09, 136.54, 133.74, 128.37, 117.43, 103.15, 66.03, 65.51, 41.41, 31.94, 29.56, 29.48, 29.35, 29.32, 26.88, 22.74, 14.19. HR-MS: *m/z* 432.2871 (observed), 432.2862 (calculated for $[M+H]^+$)

*Characterization of **11a**.* Yield: Quantitative. ^{1}H NMR (300 MHz, $CDCl_3$) δ/ppm: 10.70 (s, 1H), 7.53 (d, *J* = 7.8 Hz, 2H), 7.22 (d, *J* = 7.4 Hz, 2H), 6.17 – 5.91 (m, 1H), 5.78 (s, 1H), 5.34 (d, *J* = 17.2 Hz, 1H), 5.21 (d, *J* = 10.4 Hz, 1H), 4.62 (d, *J* = 5.5 Hz, 2H), 4.21 – 3.99 (m, 4H), 3.41 – 3.29 (m, 2H), 1.57 – 1.37 (m, 2H), 1.37 – 1.13 (m, 18H), 0.94 – 0.79 (m, 3H). ^{13}C NMR (75 MHz, $CDCl_3$) δ/ppm: 164.22, 158.64, 137.08, 136.56, 133.72, 128.34, 125.48, 117.39, 103.12, 66.00, 65.48, 41.38, 31.95, 29.67, 29.60, 29.53, 29.45, 29.39, 29.30, 26.85, 22.73, 14.17. HR-MS: *m/z* 460.3184 (observed), 460.3175 (calculated for $[M+H]^+$)

*Characterization of **12a**.* Yield: Quantitative. ^{1}H NMR (300 MHz, $CDCl_3$) δ/ppm: 10.71 (s, 1H), 7.53 (d, *J* = 7.9 Hz, 2H), 7.22 (d, *J* = 7.1 Hz, 2H), 6.11 – 5.93 (m, 1H), 5.78 (s, 1H), 5.34 (dd, *J* = 17.2, 1.2 Hz, 1H), 5.21 (dd, *J* = 10.4, 1.0 Hz, 1H), 4.61 (d, *J* = 5.6 Hz, 2H), 4.22 – 3.98 (m, 4H), 3.45 – 3.26 (m, 2H), 1.59 – 1.38 (m, 2H), 1.38 – 1.13 (m, 22H), 0.99 – 0.78 (m, 3H). ^{13}C NMR (75 MHz, $CDCl_3$) δ/ppm: 164.16, 158.61, 137.06, 136.50, 133.69, 128.30, 125.45, 117.37, 103.11, 65.98, 65.44, 41.36, 31.94, 29.70, 29.66, 29.58, 29.51, 29.43, 29.38, 29.28, 26.83, 22.71, 14.15. HR-MS: *m/z* 488.3491 (observed), 488.3488 (calculated for $[M+H]^+$)

*Characterization of **13a**.* Yield: 81%. ^{1}H NMR (300 MHz, $CDCl_3$) δ/ppm: δ 10.31 (s, 1H), 7.42 (d, *J* = 8.5 Hz, 2H), 7.01 (d, *J* = 8.4 Hz, 2H), 6.10 – 5.89 (m, 1H), 5.75 (s, 1H), 5.32 (dd, *J* = 17.2, 1.5 Hz, 1H), 5.19 (dd, *J* = 10.4, 1.3 Hz, 1H), 4.58 (dt, *J* = 5.8, 1.3 Hz, 2H), 4.21 – 3.97 (m, 4H), 3.26 (t, *J* = 7.4 Hz, 4H), 1.61 – 1.39 (m, 4H), 1.24 (h, *J* = 7.4 Hz, 4H), 0.87 (t, *J* = 7.3 Hz, 6H). ^{13}C NMR (75 MHz, $CDCl_3$) δ/ppm: 163.73, 160.90, 141.21, 133.74, 133.61, 127.87, 121.12, 117.56, 103.46, 66.25, 65.41, 48.06, 29.76, 20.12, 13.90. HR-MS: *m/z* 404.2564 (observed), 404.2549 (calculated for $[M+H]^+$)

*Characterization of **14a**.* Yield: 52%. ^{1}H NMR (300 MHz, $CDCl_3$) δ/ppm: 10.31 (s, 1H), 7.42 (d, *J* = 8.4 Hz, 2H), 7.01 (d, *J* = 8.3 Hz, 2H), 6.09 – 5.92 (m, 1H), 5.76 (s, 1H), 5.32 (dd, *J* = 17.2, 1.5 Hz, 1H), 5.20 (dd, *J* = 10.4, 1.4 Hz, 1H), 4.58 (dt, *J* = 5.8, 1.3 Hz, 2H), 4.21 – 3.97 (m, 4H), 3.35 – 3.16 (t, *J* = 7.4 Hz, 4H), 1.59 – 1.41 (m, 4H), 1.37 – 1.11 (m, 12H), 0.91 – 0.83 (m, 6H).^{13}C NMR (75 MHz, $CDCl_3$) δ/ppm: 160.93, 141.23, 133.79, 133.67, 127.89, 121.16, 117.57, 103.50, 66.28, 65.45, 48.37, 31.62, 27.64, 26.61, 22.66, 14.13. HR-MS: *m/z* 460.3200 (observed), 460.3175 (calculated for $[M+H]^+$)

*Characterization of **15a**.* Yield: Quantitative. ^{1}H NMR (300 MHz, $CDCl_3$) δ/ppm: 10.29 (s, 1H), 7.41 (d, *J* = 8.4 Hz, 2H), 7.01 (d, *J* = 8.2 Hz, 2H), 6.11 – 5.89 (m, 1H), 5.74 (s,

1H), 5.30 (dd, *J* = 17.2, 1.4 Hz, 1H), 5.17 (dd, *J* = 10.4, 1.3 Hz, 1H), 4.57 (d, *J* = 5.7 Hz, 2H), 4.18 – 3.92 (m, 4H), 3.26 (t, *J* = 7.2 Hz, 4H), 1.61 – 1.41 (m, 4H), 1.39 – 1.12 (m, 28H), 0.95 – 0.80 (m, 6H).^{13}C NMR (75 MHz, $CDCl_3$) δ/ppm: 163.40, 160.56, 140.91, 133.56, 133.40, 127.58, 120.81, 117.17, 103.17, 65.93, 65.11, 48.09, 31.73, 29.36, 29.14, 27.39, 26.64, 22.53, 13.97. HR-MS: *m/z* 572.4429 (observed), 572.4427 (calculated for $[M+H]^+$)

*Characterization of **16a**.* Yield: Quantitative. ^{1}H NMR (300 MHz, $CDCl_3$) δ/ppm: 10.72 (s, 1H), 7.52 (d, *J* = 8.2 Hz, 2H), 7.21 (d, *J* = 8.0 Hz, 2H), 6.11 – 5.92 (m, 1H), 5.78 (s, 1H), 5.34 (dd, *J* = 17.2, 1.5 Hz, 1H), 5.21 (dd, *J* = 10.4, 1.4 Hz, 1H), 5.15 (t, *J* = 5.8 Hz, 1H), 5.09 – 4.98 (m, 1H), 4.62 (d, *J* = 5.8 Hz, 2H), 4.20 – 4.00 (m, 4H), 4.02 – 3.91 (m, 2H), 2.12 – 1.91 (m, 4H), 1.65 (s, 3H), 1.63 (s, 3H), 1.58 (s, 3H). ^{13}C NMR (75 MHz, $CDCl_3$) δ/ppm: 140.53, 133.52, 131.79, 128.26, 125.27, 123.74, 119.41, 117.49, 103.13, 66.02, 65.45, 39.45, 26.27, 25.70, 17.72, 16.40. HR-MS: *m/z* 428.2556 (observed), 428.2549 (calculated for $[M+H]^+$)

*Characterization of **17a**.* Yield: 75%. ^{1}H NMR (300 MHz, $CDCl_3$) δ/ppm: 10.71 (s, 1H), 7.52 (d, *J* = 8.1 Hz, 2H), 7.23 (d, *J* = 7.4 Hz, 2H), 6.12 – 5.92 (m, 1H), 5.78 (s, 1H), 5.34 (dd, *J* = 17.2, 1.3 Hz, 1H), 5.22 (dd, *J* = 10.4, 1.3 Hz, 1H), 5.18 – 5.01 (m, 3H), 4.62 (d, *J* = 5.5 Hz, 2H), 4.19 – 4.02 (m, 4H), 4.02 – 3.92 (m, 2H), 2.14 – 1.89 (m, 8H), 1.67 (s, 3H), 1.64 (s, 3H), 1.59 (s, 3H), 1.57 (s, 3H).^{13}C NMR (75 MHz, $CDCl_3$) δ/ppm: 164.20, 158.45, 140.75, 137.12, 135.50, 133.73, 131.41, 128.36, 125.40, 124.91, 124.38, 123.72, 119.40, 117.47, 103.19, 66.07, 65.54, 39.77, 39.56, 39.50, 26.79, 26.35, 25.80, 17.80, 16.53, 16.11. HR-MS: *m/z* 496.3178 (observed), 496.3175 (calculated for $[M+H]^+$)

*Characterization of **18a**.* **18a** was used crude in the next step. The 4'-chloro-([1,1'-biphenyl]-4-yl)methanamine is present in this reaction as HCl salt. Although the reaction is performed under basic conditions in NEt_3, partial removal of the cyclic acetal and thus partial formation of **18b** was already observed in this reaction. Therefore, intermediate purification was omitted and **18a** (with partially formed **18b**) was used crude in the next step.

*Characterization of **19a**.* Yield: 91%. ^{1}H NMR (300 MHz, $CDCl_3$) δ/ppm: 10.64 (s, 1H), 7.51 (d, *J* = 8.0 Hz, 2H), 7.21 (d, *J* = 7.9 Hz, 2H), 6.14 – 5.92 (m, 1H), 5.78 (s, 1H), 5.34 (d, *J* = 17.3 Hz, 1H), 5.21 (dd, *J* = 10.4, 1.2 Hz, 1H), 4.80 (s, 1H), 4.65 (d, *J* = 5.1 Hz, 2H), 4.21 – 3.96 (m, 4H), 2.20 – 1.95 (m, 9H), 1.74 – 1.57 (m, 6H). ^{13}C NMR (75 MHz, $CDCl_3$) δ/ppm: 157.73, 137.62, 134.12, 128.37, 125.06, 117.01, 103.26, 66.46, 65.55, 42.25, 36.40, 29.65. HR-MS: *m/z* 426.2396 (observed), 426.2393 (calculated for $[M+H]^+$)

*Characterization of **20a***. Yield: 91%. ^{1}H NMR (300 MHz, $CDCl_3$) δ/ppm: 10.77 (s, 1H), 7.55 (d, *J* = 7.4 Hz, 2H), 7.25 (d, *J* = 7.1 Hz, 2H), 6.13 – 5.90 (m, 1H), 5.80 (s, 1H), 5.34 (dd, *J* = 17.2, 1.5 Hz, 1H), 5.21 (dd, *J* = 10.4, 1.3 Hz, 1H), 4.87 (s, 1H), 4.62 (d, *J* = 5.7 Hz, 2H), 4.21 – 4.00 (m, 4H), 3.10 (d, *J* = 5.4 Hz, 2H), 2.04 – 1.87 (m, 3H), 1.78 – 1.33 (m, 12H). ^{13}C NMR (75 MHz, $CDCl_3$) δ/ppm: 164.39, 159.09, 140.63, 133.82, 128.41, 125.30, 117.43, 103.21, 66.07, 65.51, 52.66, 40.36, 36.95, 33.71, 28.20. HR-MS: *m/z* 440.2541 (observed), 4440.2549 (calculated for $[M+H]^+$)

*General procedure for the synthesis of **6b-20b***. To a solution of **6a-20a** (5.8 mmol, 1 eq) in a minimal amount of THF (~10 mL), 1 M aqueous HCl (11.7 mmol, 2 eq) was added and the reaction mixture was stirred at RT for 1 h. The reaction was quenched with saturated $NaHCO_3$, and product was extracted with DCM twice. Organic layers were combined, dried over Na_2SO_4 and filtered. The crude products were concentrated under reduced pressure and where necessary purified by silica gel column chromatography (2/1 PE/EtOAc).

*Characterization of **6b***. Yield; Quantitative. ^{1}H NMR (300 MHz, CDCl3) δ/ppm: 9.86 (s, 1H), 7.82 (d, *J* = 7.9 Hz, 2H), 7.28 (d, *J* = 7.9 Hz, 2H), 6.07 – 5.86 (m, 1H), 5.33 (dd, *J* = 17.2, 1.4 Hz, 1H), 5.23 (dd, *J* = 10.4, 1.3 Hz, 1H), 4.61 (d, *J* = 5.7 Hz, 2H), 3.47 – 3.30 (m, 2H), 1.67 – 1.52 (m, 2H), 1.43 – 1.22 (m, 6H), 0.94 – 0.82 (m, 3H). ^{13}C NMR (75 MHz, CDCl3) δ/ppm: 190.84, 132.51, 131.41, 123.21, 118.14, 66.27, 41.51, 31.35, 29.08, 26.50, 22.45, 13.94. HR-MS: m/z 332.1980 (observed), 332.1974 (calculated for $[M+H]^+$)

*Characterization of **7b***. Yield: Quantitative. ^{1}H NMR (300 MHz, $CDCl_3$) δ/ppm: 9.89 (s, 1H), 7.85 (d, *J* = 8.0 Hz, 2H), 7.26 (d, *J* = 7.0 Hz, 2H), 6.05 – 5.86 (m, 1H), 5.33 (dd, *J* = 17.2, 1.4 Hz, 1H), 5.24 (dd, *J* = 10.4, 1.3 Hz, 1H), 4.61 (d, *J* = 5.8 Hz, 2H), 3.48 – 3.29 (m, 2H), 1.67 – 1.53 (m, 2H), 1.41 – 1.21 (m, 8H), 0.93 – 0.83 (m, 3H).^{13}C NMR (75 MHz, $CDCl_3$) δ/ppm: 190.91, 131.59, 123.37, 118.35, 66.41, 41.56, 31.73, 29.23, 28.96, 26.90, 22.61, 14.10. HR-MS: *m/z* 346.2138 (observed), 346.2130 (calculated for $[M+H]^+$)

*Characterization of **8b***. Yield: 98%. ^{1}H NMR (300 MHz, $CDCl_3$) δ/ppm: 9.90 (s, 1H), 7.86 (d, *J* = 8.0 Hz, 2H), 7.25 (d, *J* = 6.3 Hz, 2H), 6.10 – 5.85 (m, 1H), 5.33 (dd, *J* = 17.2, 1.4 Hz, 1H), 5.24 (dd, *J* = 10.4, 1.2 Hz, 1H), 4.61 (d, *J* = 5.8 Hz, 2H), 3.46 – 3.32 (m, 2H), 1.67 – 1.50 (m, 2H), 1.41 – 1.22 (m, 10H), 0.92 – 0.82 (m, 3H). ^{13}C NMR (75 MHz, $CDCl_3$) δ/ppm: 190.95, 131.64, 123.43, 118.40, 66.45, 41.60, 31.83, 29.28, 29.22, 26.97, 22.69, 14.16. HR-MS: *m/z* 360.2286 (observed), 360.2287 (calculated for $[M+H]^+$)

*Characterization of **9b***. Yield: 71%. ^{1}H NMR (300 MHz, $CDCl_3$) δ/ppm: 9.90 (s, 1H), 7.85 (d, *J* = 7.8 Hz, 2H), 7.25 (d, *J* = 6.2 Hz, 2H), 6.05 – 5.86 (m, 1H), 5.33 (dd, *J* =

17.2, 1.4 Hz, 1H), 5.24 (dd, *J* = 10.4, 1.3 Hz, 1H), 4.61 (d, *J* = 5.8 Hz, 2H), 3.47 – 3.28 (m, 2H), 1.68 – 1.51 (m, 2H), 1.41 – 1.18 (m, 12H), 0.92 – 0.81 (m, 3H). ^{13}C NMR (75 MHz, $CDCl_3$) δ/ppm: 190.92, 131.63, 123.41, 118.36, 66.44, 41.57, 31.89, 29.51, 29.32, 29.28, 26.96, 22.71, 14.16. HR-MS: *m/z* 374.2450 (observed), 374.2443 (calculated for $[M+H]^+$)

Characterization of ***10b***. Yield: 95%. ^{1}H NMR (300 MHz, $CDCl_3$) δ/ppm: 9.88 (s, 1H), 7.84 (d, *J* = 8.0 Hz, 2H), 7.26 (d, *J* = 7.2 Hz, 2H), 6.06 – 5.87 (m, 1H), 5.33 (dd, *J* = 17.2, 1.4 Hz, 1H), 5.23 (dd, *J* = 10.4, 1.2 Hz, 1H), 4.61 (d, *J* = 5.8 Hz, 2H), 3.45 – 3.29 (m, 2H), 1.69 – 1.52 (m, 2H), 1.42 – 1.19 (m, 14H), 0.93 – 0.83 (m, 3H).^{13}C NMR (75 MHz, $CDCl_3$) δ/ppm: 190.87, 131.56, 123.36, 118.26, 66.39, 41.55, 31.90, 29.53, 29.31, 29.29, 29.21, 26.93, 22.69, 14.14. HR-MS: *m/z* 388.2610 (observed), 388.2600 (calculated for $[M+H]^+$)

Characterization of ***11b***. Yield: 98%. ^{1}H NMR (300 MHz, $CDCl_3$) δ/ppm: 9.88 (s, 1H), 7.84 (d, *J* = 8.0 Hz, 2H), 7.26 (d, *J* = 7.2 Hz, 2H), 6.06 – 5.87 (m, 1H), 5.33 (dd, *J* = 17.2, 1.4 Hz, 1H), 5.23 (dd, *J* = 10.4, 1.2 Hz, 1H), 4.61 (d, *J* = 5.8 Hz, 2H), 3.46 – 3.27 (m, 2H), 1.69 – 1.53 (m, 2H), 1.42 – 1.17 (m, 18H), 0.94 – 0.81 (m, 3H). ^{13}C NMR (75 MHz, $CDCl_3$) δ/ppm: 190.86, 131.55, 123.34, 118.33, 66.39, 41.55, 31.92, 29.65, 29.59, 29.53, 29.36, 29.29, 29.21, 26.94, 22.70, 14.15. HR-MS: *m/z* 416.2920 (observed), 416.2913 (calculated for $[M+H]^+$)

Characterization of ***12b***. Yield: Quantitative. ^{1}H NMR (300 MHz, $CDCl_3$) δ/ppm: 9.87 (s, 1H), 7.83 (d, *J* = 8.1 Hz, 2H), 7.26 (d, *J* = 7.7 Hz, 2H), 6.05 – 5.83 (m, 1H), 5.33 (dd, *J* = 17.2, 1.5 Hz, 1H), 5.23 (dd, *J* = 10.4, 1.3 Hz, 1H), 4.61 (d, *J* = 5.8 Hz, 2H), 3.46 – 3.31 (m, 2H), 1.68 – 1.53 (m, 2H), 1.41 – 1.18 (m, 22H), 0.94 – 0.81 (m, 3H). ^{13}C NMR (75 MHz, $CDCl_3$) δ/ppm: 190.81, 131.49, 123.29, 118.27, 66.34, 41.54, 31.91, 29.64, 29.57, 29.50, 29.35, 29.27, 29.19, 26.91, 22.68, 14.12. HR-MS: *m/z* 444.3232 (observed), 444.3226 (calculated for $[M+H]^+$)

Characterization of ***13b***. Yield: 94%. ^{1}H NMR (300 MHz, $CDCl_3$) δ/ppm: 9.90 (s, 1H), 7.82 (d, *J* = 8.6 Hz, 2H), 7.07 (d, *J* = 8.4 Hz, 2H), 6.05 – 5.87 (m, 1H), 5.31 (dd, *J* = 17.2, 1.5 Hz, 1H), 5.20 (dd, *J* = 10.4, 1.4 Hz, 1H), 4.56 (dt, *J* = 5.8, 1.3 Hz, 2H), 3.34 (t, *J* = 7.5 Hz, 4H), 1.65 – 1.49 (m, 4H), 1.29 (h, *J* = 7.4 Hz, 4H), 0.90 (t, *J* = 7.3 Hz, 6H). ^{13}C NMR (75 MHz, $CDCl_3$) δ/ppm: 190.82, 133.11, 131.64, 131.51, 119.86, 117.86, 66.43, 48.26, 29.82, 20.12, 13.84. HR-MS: *m/z* 360.2294 (observed), 360.2287 (calculated for $[M+H]^+$)

Characterization of ***14b***. Yield: 88%. ^{1}H NMR (300 MHz, $CDCl_3$) δ/ppm: δ 9.90 (s, 1H), 7.82 (d, *J* = 8.6 Hz, 2H), 7.07 (d, *J* = 8.4 Hz, 2H), 6.04 – 5.88 (m, 1H), 5.31 (dd, *J* =

17.2, 1.5 Hz, 1H), 5.20 (dd, *J* = 10.4, 1.4 Hz, 1H), 4.56 (dt, *J* = 5.8, 1.3 Hz, 2H), 3.41 – 3.23 (m, 4H), 3.33 (t, *J* = 7.5 Hz, 4H), 1.35 – 1.18 (m, 12H), 0.94 – 0.79 (m, 6H). ^{13}C NMR (75 MHz, $CDCl_3$) δ/ppm: 190.82, 133.13, 131.69, 131.52, 119.90, 117.86, 66.44, 48.55, 31.51, 27.68, 26.57, 22.59, 14.07. HR-MS: *m/z* 416.2932 (observed), 416.2913 (calculated for $[M+H]^+$)

Characterization of ***15b***. Yield: 80%. ^{1}H NMR (300 MHz, $CDCl_3$) δ/ppm: 10.22 (s, 1H), 9.90 (s, 1H), 7.82 (d, *J* = 8.4 Hz, 2H), 7.07 (d, *J* = 8.0 Hz, 2H), 6.05 – 5.86 (m, 1H), 5.31 (dd, *J* = 17.2, 1.0 Hz, 1H), 5.20 (dd, *J* = 10.4, 0.9 Hz, 1H), 4.56 (d, *J* = 5.7 Hz, 2H), 3.32 (t, *J* = 7.4 Hz, 4H), 1.68 – 1.47 (m, 4H), 1.38 – 1.15 (m, 28H), 0.97 – 0.79 (m, 6H). ^{13}C NMR (75 MHz, $CDCl_3$) δ/ppm: 190.76, 133.14, 131.68, 131.50, 119.71, 117.85, 66.44, 48.54, 31.94, 29.58, 29.35, 27.72, 26.91, 22.74, 14.19. HR-MS: *m/z* 528.4174 (observed), 528.4165 (calculated for $[M+H]^+$)

Characterization of ***16b***. Yield: 77%. ^{1}H NMR (300 MHz, $CDCl_3$) δ/ppm: 9.92 (s, 1H), 7.86 (d, *J* = 8.3 Hz, 2H), 7.28 (d, *J* = 7.1 Hz, 2H), 6.06 – 5.87 (m, 1H), 5.40 – 5.19 (m, 3H), 5.10 – 5.01 (m, 1H), 4.61 (d, *J* = 5.8 Hz, 2H), 4.06 – 3.90 (m, 2H), 2.17 – 1.96 (m, 4H), 1.70 (s, 3H), 1.66 (s, 3H), 1.59 (s, 3H). ^{13}C NMR (75 MHz, $CDCl_3$) δ/ppm: 190.96, 140.97, 132.03, 131.65, 123.68, 123.16, 119.40, 66.45, 39.64, 39.54, 26.36, 25.76, 17.80, 16.52. HR-MS: *m/z* 384.2296 (observed), 384.2287 (calculated for $[M+H]^+$)

Characterization of ***17b***. Yield 40%. ^{1}H NMR (300 MHz, $CDCl_3$) δ/ppm: 9.93 (s, 1H), 7.87 (d, *J* = 8.0 Hz, 2H), 7.35 – 7.19 (m, 2H), 6.05 – 5.87 (m, 1H), 5.39 – 5.20 (m, 3H), 5.14 – 5.02 (m, 2H), 4.61 (d, *J* = 5.7 Hz, 2H), 4.05 – 3.93 (m, 2H), 2.18 – 1.91 (m, 8H), 1.71 (s, 3H), 1.67 (s, 3H), 1.59 (s, 6H). ^{13}C NMR (75 MHz, $CDCl_3$) δ/ppm: 190.96, 141.11, 135.70, 131.70, 131.48, 124.37, 123.60, 123.20, 119.39, 66.51, 39.79, 39.68, 39.60, 26.81, 26.36, 25.83, 17.82, 16.60, 16.15. HR-MS: *m/z* 452.2923 (observed), 452.2913 (calculated for $[M+H]^+$)

Characterization of ***18b***. Yield over 2 steps: 65%. ^{1}H NMR (300 MHz, $CDCl_3$) δ/ppm: 9.88 (s, 1H), 7.84 (d, *J* = 8.3 Hz, 2H), 7.59 – 7.45 (m, 4H), 7.45 – 7.34 (m, 4H), 7.19 (s, 2H), 6.05 – 5.84 (m, 1H), 5.34 (dd, *J* = 17.2, 1.2 Hz, 1H), 5.25 (dd, *J* = 10.4, 1.2 Hz, 1H), 4.68 – 4.58 (m, 4H). ^{13}C NMR (75 MHz, $CDCl_3$) δ/ppm: 190.94, 139.49, 139.12, 137.20, 133.61, 131.75, 129.06, 128.37, 128.33, 127.45, 123.61, 66.70, 45.05. HR-MS: *m/z* 448.1445 (observed), 448.1428 (calculated for $[M+H]^+$)

Characterization of ***19b***. Yield: 62%. ^{1}H NMR (300 MHz, $CDCl_3$) δ/ppm: 9.92 (s, 1H), 7.85 (d, *J* = 8.2 Hz, 2H), 7.11 (s, 2H), 6.05 – 5.79 (m, 1H), 5.32 (dd, *J* = 17.2, 1.3 Hz, 1H), 5.25 (dd, *J* = 10.4, 1.2 Hz, 1H), 4.60 (d, *J* = 5.6 Hz, 2H), 2.17 – 2.05 (m, 9H), 1.75

– 1.62 (m, 6H). ^{13}C NMR (75 MHz, $CDCl_3$) δ/ppm: 191.11, 131.84, 123.22, 66.67, 41.97, 36.49, 29.65. HR-MS: *m/z* 382.2120 (observed), 382.2131 (calculated for $[M+H]^+$)

*Characterization of **20b**.* Yield: 86%. ^{1}H NMR (300 MHz, $CDCl_3$) δ/ppm: 9.93 (s, 1H), 7.87 (d, *J* = 8.7 Hz, 2H), 7.24 (s, 2H), 6.09 – 5.80 (m, 1H), 5.34 (dd, *J* = 17.2, 1.5 Hz, 1H), 5.25 (dd, *J* = 10.4, 1.2 Hz, 1H), 4.62 (dt, *J* = 5.8, 1.3 Hz, 2H), 3.21 – 2.97 (m, 2H), 2.09 – 1.91 (m, 3H), 1.81 – 1.39 (m, 12H). ^{13}C NMR (75 MHz, $CDCl_3$) δ/ppm: 191.01, 131.73, 123.25, 66.55, 53.23, 40.48, 36.96, 33.66, 28.27. HR-MS: *m/z* 396.2271 (observed), 396,2287 (calculated for $[M+H]^+$)

*General procedure for the synthesis of **6c-20c**.* To a solution of **6b**-**20b** (538 µmol, 2 eq) in DMF/MeOH (4 mL), vancomycin hydrochloride (269 µmol, 1 eq) and DIPEA (1.35 mmol, 5 eq) were added. After the reaction was stirred under reflux conditions at 70 ºC for 2 h, $NaBH_3CN$ (2.69 mmol, 10 eq) was added and the reaction temperature was reduced to 50 ºC. After 5 h, an additional 10 eq of $NaBH_3CN$ (2.69 mmol) was added, followed 18 h after by an extra 10 eq $NaBH_3CN$ (2.69 mmol) and 1 eq of **6b-20b** (269 µmol). After an additional 18 h, the reaction mixture was quenched by the addition of H_2O. Solvents were evaporated under reduced pressure, the residue was redissolved in DMF and precipitated twice in cold diethyl ether. The precipitates were dried and used crude in the next step.

*General procedure for the synthesis of **6-20**.* To a solution of crude **6c-20c** (269 µmol, 1 eq) in dry DMF (5 mL) under argon atmosphere, $Pd(PPh_3)_4$ (67 µmol, 0.25 eq) and phenylsilane (6.7 mmol, 25 eq) were added. The reaction mixture was stirred for 1 h at RT under argon atmosphere. After complete deprotection, the reaction was quenched with H_2O and the solvents were evaporated under reduced pressure. The residue was redissolved in a mixture of buffer A (50 mM ammonium acetate) and buffer B (95% CH_3CN, 5% H_2O) and centrifuged to remove any residual solids. The supernatant was applied to preparative RP-HPLC using different gradients of buffer A to B based on the compound's polarity. The purity of the fractions was assessed on analytical RP-HPLC using a 0-100% buffer B gradient over 30 minutes. Pure fractions were pooled and lyophilized to obtain a white powder. The purity of the pooled final compound was assessed on analytical RP-HPLC using a 0-100% buffer B gradient over 60 minutes. See **Table 6** for HRMS analysis and yields, see **Figure S1** for chromatographic plots and final purities of the guanidino lipoglycopeptides.

Table 6. HRMS analysis and yields of the guanidino lipoglycopeptides.

Sample ID	Chemical formula	Calculated M + H	Calculated (M+2H)/2	Measured	Yield over 2 steps
6	$C_{80}H_{96}Cl_2N_{12}O_{24}$	1679.6115	840.3097	840.3100	54%
7	$C_{81}H_{98}Cl_2N_{12}O_{24}$	1693.6272	847.3175	847.3168	43%
8	$C_{82}H_{100}Cl_2N_{12}O_{24}$	1707.6428	854.3253	854.3256	5%
9	$C_{83}H_{102}Cl_2N_{12}O_{24}$	1721.6585	861.3332	861.3334	74%
10	$C_{84}H_{104}Cl_2N_{12}O_{24}$	1735.6741	868.3410	868.3418	13%
11	$C_{86}H_{108}Cl_2N_{12}O_{24}$	1763.7054	882.3566	882.3573	16%
12	$C_{88}H_{112}Cl_2N_{12}O_{24}$	1791.7367	896.3723	896.3725	5%
13	$C_{82}H_{100}Cl_2N_{12}O_{24}$	1707.6429	854.3254	854.3265	33%
14	$C_{86}H_{108}Cl_2N_{12}O_{24}$	1763.7055	882.3567	882.3561	34%
15	$C_{94}H_{124}Cl_2N_{12}O_{24}$	1875.8306	938.4192	938.4197	9%
16	$C_{84}H_{100}Cl_2N_{12}O_{24}$	1731.6428	866.3253	866.3254	34%
17	$C_{89}H_{108}Cl_2N_{12}O_{24}$	1799.7054	900.3566	900.3564	11%
18	$C_{87}H_{93}Cl_3N_{12}O_{24}$	1795.5569	898.2824	898.2828	15%
19	$C_{84}H_{98}Cl_2N_{12}O_{24}$	1729.6272	865.3175	1729.6245	9%
20	$C_{85}H_{100}Cl_2N_{12}O_{24}$	1743.6429	872.3253	1743.6435	9%

2.4.2 *In vitro* activity assessment

Bacterial strains. All ATCC reference strains were commercially obtained or supplied by the LUMC, Leiden. The *E. faecium* and *E. faecalis* strains were clinical isolates obtained from the UMCU, Utrecht. MRSA USA300 is a clinical isolate from the Texas Children's Hospital. The other *S. aureus* clinical isolates (MRSA, VISA, and VRSA) were supplied by the Network on Antimicrobial Resistance in *S. aureus* (NARSA) via BEI Resources, NIAID, NIH.

Broth microdilution assay. From glycerol stocks, bacterial strains were cultured on blood agar plates and incubated overnight at 37 °C. A single colony was transferred to tryptic soy broth (TSB) with 0.002% polysorbate 80 (p80). In case of VRSA strains, 6 μg/mL vancomycin was supplemented to the media. The cultures were grown to exponential phase (OD_{600}=0.5) at 37 °C. The bacterial suspensions were diluted 100-fold in TSB with 0.002% p80 (no vancomycin was supplemented to the media of VRSA from here on) and 50 μL was added to a 2-fold serial dilution series of test compound (50 μL per well) in polypropylene 96-well microtiter plates to reach a volume of 100 μL. The plates were sealed with breathable membranes and incubated at 37 °C for 20-24 h with constant shaking (600 rpm). For *S. pneumoniae* direct colony suspension was used by immediately suspending multiple colonies from fresh blood agar plates in TSB + 0.002% p80 to an OD_{600} of 0.5 and subsequent 100-fold dilution in TSB + 0.002% p80 + 5% lysed horse blood. Antibiotic dilutions for this strain were also made in TSB + 0.002% p80 + 5% lysed horse blood. Both agar and microplates containing *S. pneumoniae* were incubated at 37 °C with 5% CO_2 for 24 h with constant shaking (600 rpm). The MICs were

determined from the median of a minimum of triplicates. For determination of the MIC_{50} and MIC_{90} of the guanidino lipoglycopeptides, the MIC values of a panel of strains was assessed. The MIC_{50} and MIC_{90} values were based on the concentrations at which growth was visibly inhibited for 50% and 90% of the strains tested respectively. MIC testing for *Clostridium* species was performed by NIZO. Similar procedures as described above were followed, with some adjustments. As medium, brain-heart infusion medium was used. Furthermore, cultures were grown until OD_{625} = 0.8-1 and subsequently diluted to achieve a final concentration of 10^6 cells per well once 10 µL of cells was added to 50 µL of compound serial dilutions. Plates were sealed with sticky foil and incubated at 37 °C under anaerobic conditions for 24 h for *C. difficile* and *C. perfringens* and 48 h for *C. sporogenes* and *C. tyrobutyricum*.

2.5 Supplementary Information

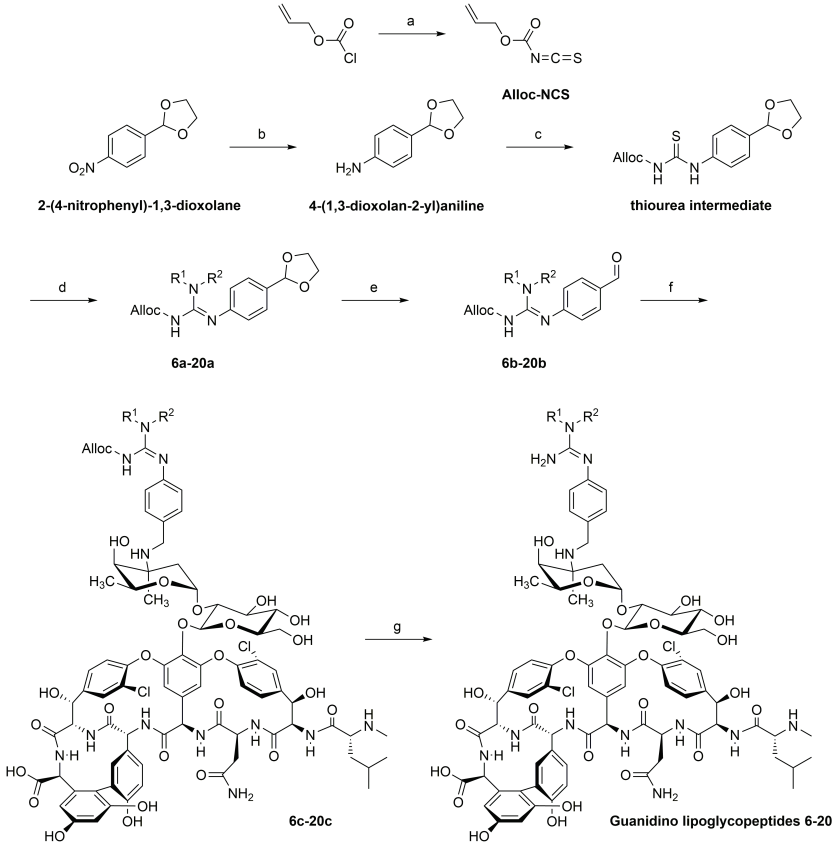

Scheme S1. General synthetic route of the guanidino lipoglycopeptides 6-20. a) KNCS, 18-crown-6, CCl_4, 90 °C; b) H_2, PtO_2, $NaHCO_3$, EtOH, RT; c) Alloc-NCS, DIPEA, CH_2Cl_2, RT; d) NR_1R_2, NEt_3, EDC HCl, CH_2Cl_2, RT; e) HCl, THF/H_2O, RT; f) Vancomycin HCl, DIPEA, $NaBH_3CN$, DMF/MeOH, 50 °C; g) $Pd(PPh_3)_4$, phenylsilane, DMF, RT.

Table S1. Extended *in vitro* activity of the guanidino lipoglycopeptides against Gram positive strains.

Compound		MIC (μg/mL) Strain				
Id	**Structure**	**MRSA[a]**	**VISA[b]**	**VRSA[c]**	**VRE (VanA)[d]**	**VRE (VanB)[e]**
1	Vancomycin	2	8	>128	>128	16
2	Teicoplanin	0.5	4	16	>128	0.125
3	Telavancin	0.031	0.25	8	4	0.063
4	Dalbavancin	≤0.008	0.5	2	>128	0.031
5	Oritavancin	0.25	4	0.25	1	0.063
Guanidino lipoglycopeptides						
6	$-C_6H_{13}$	0.063	0.5	16	32	0.25
7	$-C_7H_{15}$	≤0.008	0.063	8	16	0.016
8	$-C_8H_{17}$	≤0.008	≤0.008	2	8	≤0.008
9	$-C_9H_{19}$	≤0.008	≤0.008	0.5	2	≤0.008
10	$-C_{10}H_{21}$	≤0.008	0.063	0.25	1	≤0.008
11	$-C_{12}H_{25}$	0.5	0.25	0.25	1	0.063
12	$-C_{14}H_{29}$	8	2	1	2	1
13	$-C_4H_9$ $-C_4H_9$	0.063	1	64	>128	8
14	$-C_6H_{13}$ $-C_6H_{13}$	≤0.008	0.063	1	8	≤0.008
15	$-C_{10}H_{21}$ $-C_{10}H_{21}$	16	16	8	32	4
16	-Ger[f]	≤0.008	0.031	1	8	≤0.008
17	-Far[g]	0.125	0.125	0.5	1	0.031
18	$-CH_2$-CBP[h]	≤0.008	0.031	0.5	1	≤0.008
19	-TCD[i]	0.031	≤0.016	8	16	0.125
20	$-CH_2$-TCD[i]	≤0.008	≤0.016	2	16	≤0.008

MIC values are the median of a minimum of triplicates. MIC = minimum inhibitory concentration. [a]Methicillin-resistant *S. aureus* NY-155, NR-46236. [b]Vancomycin-sensitive *S. aureus* HIP12864, NR-46074. [c]Vancomycin-resistant (VanA) *S. aureus* 880 (BR-VRSA), NR-49120. [d]Vancomycin-resistant (VanA) *Enterococcus faecalis* E1246. [e]Vancomycin-resistant (VanB) *E. faecalis* E7604. [f]Ger = geranyl. [g]Far = farnesyl. [h]CBP = 4-chloro-1,1'-biphenyl. [i]TCD = tricyclo[3.3.1.1^{3,7}]decane or adamantane.

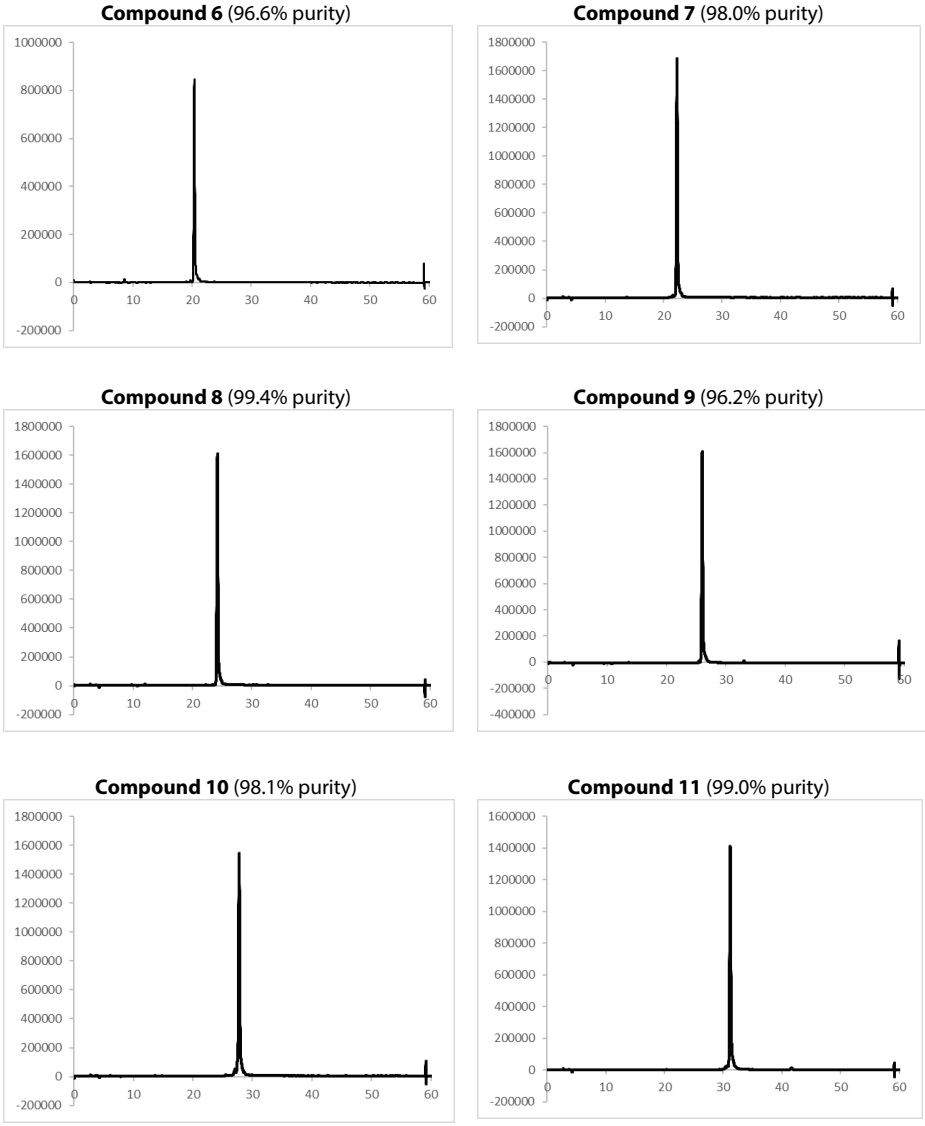

Fig. S1. Purity of the guanidino lipoglycopeptides

Compound 12 (98.7% purity)

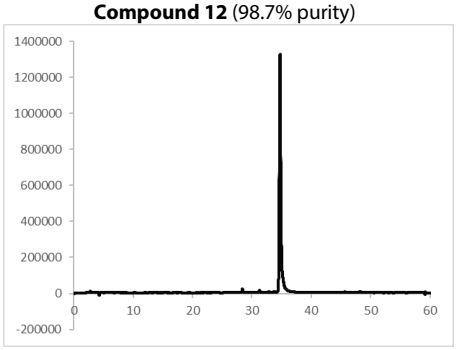

Compound 13 (94.6% purity)

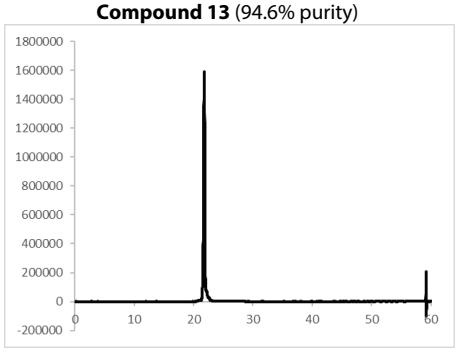

Compound 14 (95.7% purity)

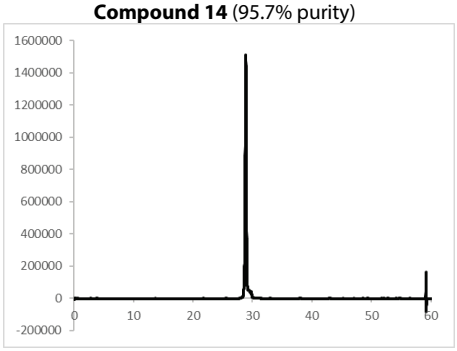

Compound 15 (97.7% purity)

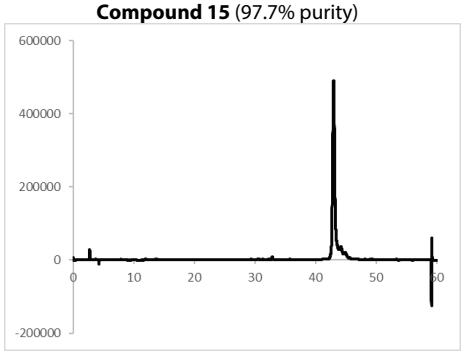

Compound 16 (98.9% purity)

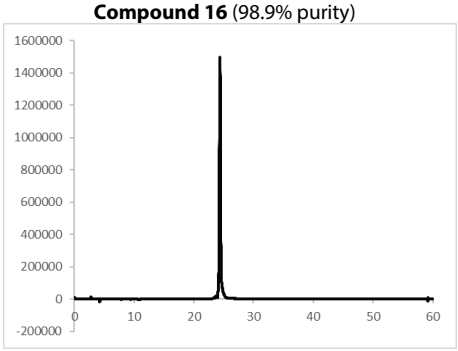

Compound 17 (96.6% purity)

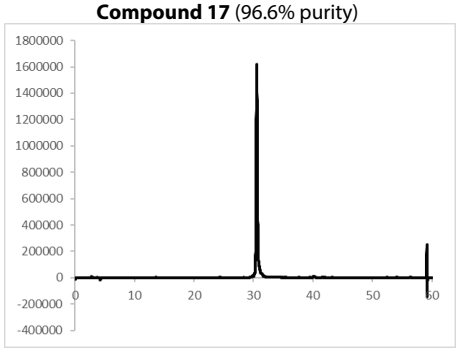

Fig. S1. Purity of the guanidino lipoglycopeptides (continued)

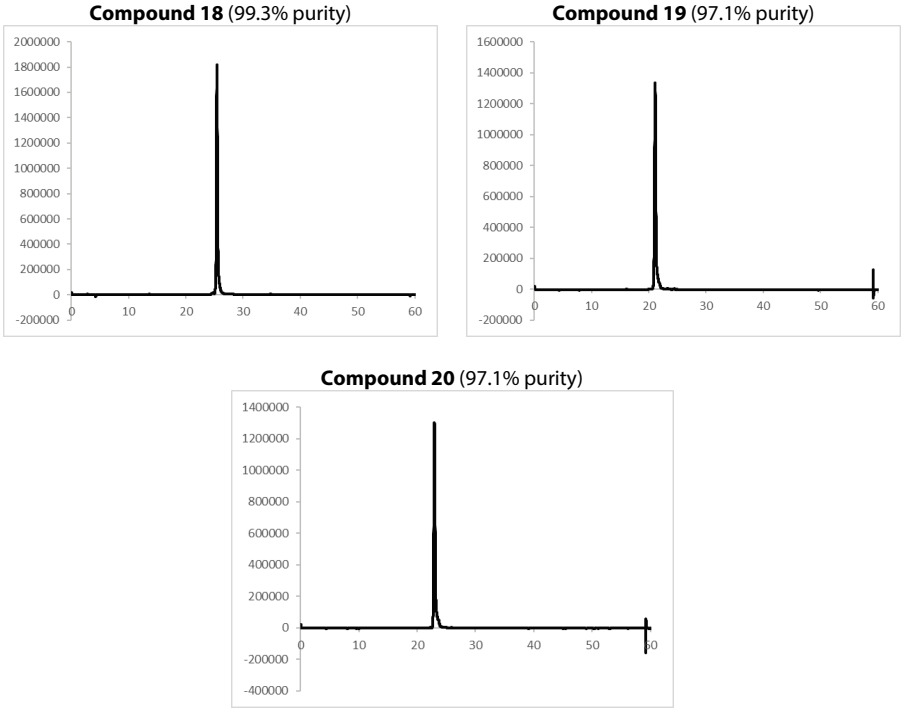

Fig. S1. Purity of the guanidino lipoglycopeptides (continued)

References

1. WHO. *Antimicrobial Resistance Global Report on Surveillance*. (2014).
2. Centers for Disease Control (US). *Antibiotic Resistance Threats in the United States, 2019*. www.cdc.gov/DrugResistance/Biggest-Threats.html. (2019).
3. McGuinness, W. A., Malachowa, N. & Deleo, F. R. Vancomycin Resistance in Staphylococcus aureus. *Yale J. Biol. Med.* **90**, 269–281 (2017).
4. Van Hal, S. J. & Fowler Jr, V. G. Is It Time to Replace Vancomycin in the Treatment of Methicillin-Resistant Staphylococcus aureus Infections? *Clin. Infect. Dis.* **56**, 1779–1788 (2013).
5. Cassini, A., *et al.* Attributable deaths and disability-adjusted life-years caused by infections with antibiotic-resistant bacteria in the EU and the European Economic Area in 2015: a population-level modelling analysis. *Lancet Infect. Dis.* **19**, 56–66 (2019).
6. Murray, C. J. L., *et al.* Global burden of bacterial antimicrobial resistance in 2019: a systematic analysis. *Lancet* **399**, 629–655 (2022).
7. Pootoolal, J., Neu, J. & Wright, G. D. Glycopeptide Antibiotic Resistance. *Annu. Rev. Pharmacol. Toxicol.* **42**, 381–408 (2002).
8. Walsh, C. T., Fisher, S. L., Park, I. S., Prahalad, M. & Wu, Z. Bacterial resistance to vancomycin: Five genes and one missing hydrogen bond tell the story. *Chem. Biol.* **3**, 21–28 (1996).
9. Blaskovich, M. A. T., Hansford, K. A., Butler, M. S., Jia, Z., Mark, A. E. & Cooper, M. A. Developments in Glycopeptide Antibiotics. *ACS Infect. Dis.* **4**, 715–735 (2018).
10. Barna, J. C. & Williams, D. H. The structure and mode of action of glycopeptide antibiotics of the vancomycin group. *Annu. Rev. Microbiol.* **38**, 339–357 (1984).
11. McComas, C. C., Crowley, B. M. & Boger, D. L. Partitioning the Loss in Vancomycin Binding Affinity for d-Ala-d-Lac into Lost H-Bond and Repulsive Lone Pair Contributions. *J. Am. Chem. Soc.* **125**, 9314–9315 (2003).

12. Bugg, T. D. H., Wright, G. D., Dutka-Malen, S., Arthur, M., Courvalin, P. & Walsh, C. T. Molecular basis for vancomycin resistance in Enterococcus faecium BM4147: biosynthesis of a depsipeptide peptidoglycan precursor by vancomycin resistance proteins VanH and VanA. *Biochemistry* **30**, 10408–10415 (1991).
13. Arthur, M. & Quintiliani, R. Regulation of VanA-and VanB-type glycopeptide resistance in enterococci. *Antimicrob. Agents Chemother.* **45**, 375–381 (2001).
14. Courvalin, P. Resistance of enterococci to glycopeptides. *Antimicrob. Agents Chemother.* **34**, 2291–2296 (1990).
15. Cui, L., Ma, X., Sato, K., Okuma, K., Tenover, F. C., Mamizuka, E. M., Gemmell, C. G., Kim, M.-N., Ploy, M.-C., Solh, N. El, Ferraz, V. & Hiramatsu, K. Cell Wall Thickening Is a Common Feature of Vancomycin Resistance in Staphylococcus aureus. *J. Clin. Microbiol.* **41**, 5–14 (2003).
16. Howden, B. P., Davies, J. K., Johnson, P. D. R., Stinear, T. P. & Lindsay Grayson, M. Reduced Vancomycin Susceptibility in Staphylococcus aureus, Including Vancomycin-Intermediate and Heterogeneous Vancomycin-Intermediate Strains: Resistance Mechanisms, Laboratory Detection, and Clinical Implications. *Clin. Microbiol. Rev.* **23**, 99–139 (2010).
17. Hayden, M. K., Rezai, K., Hayes, R. A., Lolans, K., Quinn, J. P. & Weinstein, R. A. Development of Daptomycin Resistance In Vivo in Methicillin-Resistant Staphylococcus aureus. *J. Clin. Microbiol.* **43**, 5285–5287 (2005).
18. Tran, T. T., Munita, J. M. & Arias, C. A. Mechanisms of drug resistance: Daptomycin resistance. *Ann. N. Y. Acad. Sci.* **1354**, 32–53 (2015).
19. Gu, B., Kelesidis, T., Tsiodras, S., Hindler, J. & Humphries, R. M. The emerging problem of linezolid-resistant Staphylococcus. *J. Antimicrob. Chemother.* **68**, 4–11 (2013).
20. Gonzales, R. D., Schreckenberger, P. C., Beth Graham, M., Kelkar, S., DenBesten, K. & Quinn, J. P. Infections due to vancomycin-resistant Enterococcus faecium resistant to linezolid. *Lancet* **357**, 1179 (2001).
21. Barriere, S. L. The ATTAIN trials: Efficacy and safety of telavancin compared with vancomycin for the treatment of hospital-acquired and ventilator-associated bacterial pneumonia. *Future Microbiol.* **9**, 281–289 (2014).
22. Zhanel, G. G., Calic, D., Schweizer, F., Zelenitsky, S., Adam, H., Lagacé-Wiens, P. R. S., Rubinstein, E., Gin, A. S., Hoban, D. J. & Karlowsky, J. A. New lipoglycopeptides: a comparative review of dalbavancin, oritavancin and telavancin. *Drugs* **70**, 859–886 (2010).
23. Stein, G. E. Oritavancin: A Long-Half-Life Lipoglycopeptide. *Clin. Infect. Dis.* **61**, 627–632 (2015).
24. The Medicines Company. Prescribing information for ORBACTIV (oritavancin) for injection, for intravenous use. http://www.orbactiv.com/pdfs/orbactiv-prescribing-information.pdf (2021).
25. Karlowsky, J. A., Nichol, K. & Zhanel, G. G. Telavancin: Mechanisms of Action, In Vitro Activity, and Mechanisms of Resistance. *Clin. Infect. Dis.* **61**, S58–S68 (2015).
26. Cada, D. J. & Baker, D. E. Oritavancin diphosphate. *Hosp. Pharm.* **49**, 1049–1060 (2014).
27. Yarlagadda, V., Akkapeddi, P., Manjunath, G. B. & Haldar, J. Membrane active vancomycin analogues: A strategy to combat bacterial resistance. *J. Med. Chem.* **57**, 4558–4568 (2014).
28. Okano, A., Nakayama, A., Wu, K., Lindsey, E. A., Schammel, A. W., Feng, Y., Collins, K. C. & Boger, D. L. Total Syntheses and Initial Evaluation of [Ψ[C(═S)NH]Tpg4]vancomycin, [Ψ[C(═NH)NH]Tpg4]vancomycin, [Ψ[CH2NH]Tpg4]vancomycin, and Their (4-Chlorobiphenyl)methyl Derivatives: Synergistic Binding Pocket and Peripheral Modifications for the Glycopeptide Antib. *J. Am. Chem. Soc.* **137**, 3693–3704 (2015).
29. Xie, J., Okano, A., Pierce, J. G., James, R. C., Stamm, S., Crane, C. M. & Boger, D. L. Total Synthesis of [Ψ[C(═S)NH]Tpg4]Vancomycin Aglycon, [Ψ[C(═NH)NH]Tpg4]Vancomycin Aglycon, and Related Key Compounds: Reengineering Vancomycin for Dual d-Ala-d-Ala and d-Ala-d-Lac Binding. *J. Am. Chem. Soc.* **134**, 1284–1297 (2012).
30. Crowley, B. M. & Boger, D. L. Total synthesis and evaluation of [Ψ[CH2NH]Tpg4]vancomycin aglycon: reengineering vancomycin for dual D-Ala-D-Ala and D-Ala-D-Lac binding. *J. Am. Chem. Soc.* **128**, 2885–2892 (2006).
31. Okano, A., James, R. C., Pierce, J. G., Xie, J. & Boger, D. L. Silver(I)-Promoted Conversion of Thioamides to Amidines: Divergent Synthesis of a Key Series of Vancomycin Aglycon Residue 4 Amidines That Clarify Binding Behavior to Model Ligands. *J. Am. Chem. Soc.* **134**, 8790–8793 (2012).
32. Okano, A., Nakayama, A., Schammel, A. W. & Boger, D. L. Total synthesis of [Ψ[C(═NH)NH]Tpg(4)]vancomycin and its (4-chlorobiphenyl)methyl derivative: impact of peripheral modifications on vancomycin analogues redesigned for dual D-Ala-D-Ala and D-Ala-D-

Lac binding. *J. Am. Chem. Soc.* **136**, 13522–13525 (2014).
33. Antonoplis, A., Zang, X., Wegner, T., Wender, P. A. & Cegelski, L. Vancomycin-Arginine Conjugate Inhibits Growth of Carbapenem-Resistant E. coli and Targets Cell-Wall Synthesis. *ACS Chem. Biol.* **14**, 2065–2070 (2019).
34. Neville, L., Shalit, I., Warn, P. A., Scheetz, M. H., Sun, J., Chosy, M. B., Wender, P. A., Cegelski, L. & Rendell, J. T. In Vivo Targeting of Escherichia coli with Vancomycin-Arginine. *Antimicrob. Agents Chemother.* **65**, e02416-20 (2022).
35. Sarkar, P., Samaddar, S., Ammanathan, V., Yarlagadda, V., Ghosh, C., Shukla, M., Kaul, G., Manjithaya, R., Chopra, S. & Haldar, J. Vancomycin Derivative Inactivates Carbapenem-resistant Acinetobacter baumannii and Induces Autophagy. *ACS Chem. Biol.* **15**, 884–889 (2020).
36. Guan, D., Chen, F., Qiu, Y., Jiang, B., Gong, L., Lan, L. & Huang, W. Sulfonium, an Underestimated Moiety for Structural Modification, Alters the Antibacterial Profile of Vancomycin Against Multidrug-Resistant Bacteria. *Angew. Chemie Int. Ed.* **58**, 6678–6682 (2019).
37. Umstätter, F., Domhan, C., Hertlein, T., Ohlsen, K., Mühlberg, E., Kleist, C., Zimmermann, S., Beijer, B., Klika, K. D., Haberkorn, U., Mier, W. & Uhl, P. Vancomycin Resistance Is Overcome by Conjugation of Polycationic Peptides. *Angew. Chemie Int. Ed.* **59**, 8823–8827 (2020).
38. Yarlagadda, V., Samaddar, S., Paramanandham, K., Shome, B. R. & Haldar, J. Membrane Disruption and Enhanced Inhibition of Cell-Wall Biosynthesis: A Synergistic Approach to Tackle Vancomycin-Resistant Bacteria. *Angew. Chemie Int. Ed.* **54**, 13644–13649 (2015).
39. Sarkar, P., Basak, D., Mukherjee, R., Bandow, J. E. & Haldar, J. Alkyl-Aryl-Vancomycins: Multimodal Glycopeptides with Weak Dependence on the Bacterial Metabolic State. *J. Med. Chem.* **64**, 10185–10202 (2021).
40. Blaskovich, M. A. T., *et al.* Protein-inspired antibiotics active against vancomycin- and daptomycin-resistant bacteria. *Nat. Commun.* **9**, 1–17 (2018).
41. Wu, Z.-C., Cameron, M. D. & Boger, D. L. Vancomycin C-Terminus Guanidine Modifications and Further Insights into an Added Mechanism of Action Imparted by a Peripheral Structural Modification. *ACS Infect. Dis.* **6**, 2169–2180 (2020).
42. Okano, A., Isley, N. A. & Boger, D. L. Peripheral modifications of [Ψ[CH 2 NH]Tpg 4]vancomycin with added synergistic mechanisms of action provide durable and potent antibiotics. *Proc. Natl. Acad. Sci.* **114**, 5052–5061 (2017).
43. van Groesen, E., Slingerland, C. J., Innocenti, P., Mihajlovic, M., Masereeuw, R. & Martin, N. I. Vancomyxins: Vancomycin-Polymyxin Nonapeptide Conjugates That Retain Anti-Gram-Positive Activity with Enhanced Potency against Gram-Negative Strains. *ACS Infect. Dis.* **7**, 2746–2754 (2021).
44. Shi, W., Chen, F., Zou, X., Jiao, S., Wang, S., Hu, Y., Lan, L., Tang, F. & Huang, W. Design, synthesis, and antibacterial evaluation of vancomycin-LPS binding peptide conjugates. *Bioorg. Med. Chem. Lett.* **45**, 128122 (2021).
45. Xie, J., Pierce, J. G., James, R. C., Okano, A. & Boger, D. L. A Redesigned Vancomycin Engineered for Dual d-Ala-d-Ala and d-Ala-d-Lac Binding Exhibits Potent Antimicrobial Activity Against Vancomycin-Resistant Bacteria. *J. Am. Chem. Soc.* **133**, 13946–13949 (2011).
46. Van Haren, M. J., Marechal, N., Troffer-Charlier, N., Cianciulli, A., Sbardella, G., Cavarelli, J. & Martin, N. I. Transition state mimics are valuable mechanistic probes for structural studies with the arginine methyltransferase CARM1. *Proc. Natl. Acad. Sci.* **114**, 3625–3630 (2017).
47. Mooney, C. A., Johnson, S. A., 'T Hart, P., Quarles Van Ufford, L., De Haan, C. A. M., Moret, E. E. & Martin, N. I. Oseltamivir analogues bearing N-substituted guanidines as potent neuraminidase inhibitors. *J. Med. Chem.* **57**, 3154–3160 (2014).
48. Sevšek, A., Sastre Toraño, J., Quarles van Ufford, L., Moret, E. E., Pieters, R. J. & Martin, N. I. Orthoester functionalized N-guanidino derivatives of 1,5-dideoxy-1,5-imino-d-xylitol as pH-responsive inhibitors of β-glucocerebrosidase. *Medchemcomm* **8**, 2050–2054 (2017).
49. Zhang, Y., van Haren, M. J. & Martin, N. I. Peptidic transition state analogues as PRMT inhibitors. *Methods* **175**, 24–29 (2020).
50. Kouhsari, E., Abbasian, S., Sedighi, M., Yaseri, H. F., Nazari, S., Bialvaei, A. Z., Dahim, P., Mirzaei, E. Z. & Rahbar, M. Clostridium difficile infection: a review. *Rev. Med. Microbiol.* **29**, 103–109 (2018).
51. Peng, Z., Jin, D., Kim, H. B., Stratton, C. W., Wu, B., Tang, Y.-W. & Sun, X. Update on Antimicrobial Resistance in Clostridium difficile: Resistance Mechanisms and Antimicrobial Susceptibility Testing. *J. Clin. Microbiol.* **55**, 1998–2008 (2017).
52. Goudarzi, M., Goudarzi, H., Alebouyeh, M., Azimi Rad, M., Shayegan Mehr, F. S., Zali, M. R. &

Aslani, M. M. Antimicrobial susceptibility of clostridium difficile clinical isolates in iran. *Iran. Red Crescent Med. J.* **15**, 704–711 (2013).
53. Polage, C. R., Solnick, J. V & Cohen, S. H. Nosocomial Diarrhea: Evaluation and Treatment of Causes Other Than Clostridium difficile. *Clin. Infect. Dis.* **55**, 982–989 (2012).
54. Lee, J., Jang, Y.-S., Han, M.-J., Kim, J. Y., Lee, S. Y., Katze, M. G., Li, Y. & Soucaille, P. Deciphering Clostridium tyrobutyricum Metabolism Based on the Whole-Genome Sequence and Proteome Analyses. *MBio* **7**, e00743-16 (2016).
55. Peck, M. W. & van Vliet, A. H. M. Impact of Clostridium botulinum genomic diversity on food safety. *Curr. Opin. Food Sci.* **10**, 52–59 (2016).
56. Schill, K. M., Wang, Y., Butler, R. R., Pombert, J.-F., Reddy, N. R., Skinner, G. E., Larkin, J. W. & Schaffner, D. W. Genetic Diversity of Clostridium sporogenes PA 3679 Isolates Obtained from Different Sources as Resolved by Pulsed-Field Gel Electrophoresis and High-Throughput Sequencing. *Appl. Environ. Microbiol.* **82**, 384–393 (2016).
57. Ghosh, M., Miller, P. A. & Miller, M. J. Antibiotic repurposing: bis-catechol- and mixed ligand (bis-catechol-mono-hydroxamate)-teicoplanin conjugates are active against multidrug resistant Acinetobacter baumannii. *J. Antibiot.* **73**, 152–157 (2020).
58. Ghosh, M. & Miller, M. J. Synthesis and in vitro antibacterial activity of spermidine-based mixed catechol- and hydroxamate-containing siderophore--vancomycin conjugates. *Bioorg. Med. Chem.* **4**, 43–48 (1996).
59. Levine, D. P. Vancomycin: A History. *Clin. Infect. Dis.* **42**, S5–S12 (2006).
60. Martin, N. I., Woodward, J. J. & Marletta, M. A. NG-hydroxyguanidines from primary amines. *Org. Lett.* **8**, 4035–4038 (2006).
61. Hughes, A., Byun, D., Chen, Y., Fleury, M., Jacobsen, J. R., Stangeland, E., Wilson, R. D. & Yen, R. WO2010123766 - Diamide compounds having muscarinic receptor antagonist and β2 andrenergic receptor agonist activity. (2010).
62. Zahn, T. J., Eilers, M., Guo, Z., Ksebati, M. B., Simon, M., Scholten, J. D., Smith, S. O. & Gibbs, R. A. Evaluation of Isoprenoid Conformation in Solution and in the Active Site of Protein-Farnesyl Transferase Using Carbon-13 Labeling in Conjunction with Solution- and Solid-State NMR. *J. Am. Chem. Soc.* **122**, 7153–7164 (2000).
63. Xie, H., Shao, Y., Becker, J. M., Naider, F. & Gibbs, R. A. Synthesis and Biological Evaluation of the Geometric Farnesylated Analogues of the a-Factor Mating Peptide of Saccharomyces cerevisiae. *J. Org. Chem.* **65**, 8552–8563 (2000).
64. Koopmans, T., Wood, T. M., 't Hart, P., Kleijn, L. H. J., Hendrickx, A. P. A., Willems, R. J. L., Breukink, E. & Martin, N. I. Semisynthetic Lipopeptides Derived from Nisin Display Antibacterial Activity and Lipid II Binding on Par with That of the Parent Compound. *J. Am. Chem. Soc.* **137**, 9382–9389 (2015).
65. Coppola, G. M. & Prashad, M. A Convenient Preparation of Farnesylamine. *Synth. Commun.* **23**, 535–541 (1993).